Designing biocompatible protein nanoparticles for improving the cellular uptake and antioxidation activity of tetrahydrocurcumin

by Chen, S., Wu, Q., Ma, M., Huang, Z., Vriesekoop, F. and Liang, H.

Copyright, publisher and additional Information: This is the author accepted manuscript. The final published version (version of record) is available online via Elsevier.
This version is made available under the CC-BY-ND-NC licence

Please refer to any applicable terms of use of the publisher

DOI link to the version of record on the publisher's website

Chen, S., Wu, Q., Ma, M., Huang, Z., Vriesekoop, F. and Liang, H. 2021. Designing biocompatible protein nanoparticles for improving the cellular uptake and antioxidation activity of tetrahydrocurcumin. *Journal of Drug Delivery Science and Technology*, *63*.

18 February 2021

Journal of Drug Delivery Science and Technology

Designing biocompatible protein nanoparticles for improving the cellular uptake and antioxidation activity of Tetrahydrocurcumin.

--Manuscript Draft--

Manuscript Number:	JDDST-D-20-00777R1
Article Type:	Research Paper
Keywords:	Sodium caseinate; Tetrahydrocurcumin; nanoparticles; Cellular uptake; Antioxidant
Corresponding Author:	Hao Liang CHINA
First Author:	Shan Chen
Order of Authors:	Shan Chen
	Qiao Wu
	Mengyan Ma
	Zezhong Huang
	Hao Liang
	Frank Vriesekoop
Abstract:	Tetrahydrocurcumin (THC) is a natural molecule with anticancerous, antioxidant and other beneficial activities. However, its low aqueous solubility leads to poor bioavailability. Sodium caseinate (NaCas) is an ideal natural protein carrier with amphiphilic and non-toxic properties, which provides a new possibility for improving the aqueous solubility of THC. In this study, THC loaded protein nanoparticles (THC@NaCas) were successfully prepared by a nanoprecipitation method. The protein-based carrier awarded an encapsulation efficiency of about 98% for THC. The structure and physicochemical characteristics of THC@NaCas nanoparticles were characterized by Fourier Transform Infrared Spectroscopy (FTIR), X-ray diffraction, and Scanning Electron Microscopy (SEM). The solubility test comfirmed that protein nanoparticles awarded greater solubility of THC. Furthermore, THC@NaCas had a greater antioxidant activity compared to free THC, resulting in a free radical scavenging ability of THC@NaCas 2.6 times greater than that of free THC. The in vitro cytotoxicity test showed that the THC@NaCas nanoparticles had a stronger inhibitory effect on cancer cells compared with free THC, and good biocompatibility for non-cancerous cells. In a short, Our results demonstrate that protein-based nanoparticles have the potential to improve the bioactivity of hydrophobic drugs in clinical application.
Suggested Reviewers:	Jin-Ye Wang jinyewang@sjtu.edu.cn
	Yern Chee Ching chigyc@um.edu.my
	Takahiro Suzuki tsuzuki@hmc.hosokawa.com
	Aizong Shen sazljl@126.com
Opposed Reviewers:	
Response to Reviewers:	Thank you giving some suggestions about our manuscript.

Powered by Editorial Manager® and ProduXion Manager® from Aries Systems Corporation

Dear Editors:

Thank you very much for giving us a chance to revise our manuscript. We have carefully read the Referees' comments. Those comments are all valuable and very helpful for revising and improving our paper, as well as the important guiding significance to our researches. We have modified our manuscript and a point-by-point response to the reviewers' comments was given in another file (Responses to Reviewers). Meanwhile, we also updated a version of our manuscript and supplement file with red mark.

In this paper, we designed a biocompatible protein nanoparticle to improve the antioxidation and cellular uptake of tetrahydrocurcumin (THC). THC@NaCas nanoparticles were synthesized by employing a simple, ecofriendly, and economical coacervation technique. The encapsulation of THC in NaCas greatly improved the antioxidant activity, the cellular uptake and the inhibition activity on tyrosinase of THC. Our results reveal that the protein nanoparticles have the potential to improve the bioactivity of hydrophobic drugs in clinical application.

This revise manuscript contain about 7017 words, 47 references and 8 figures.

We deeply appreciate your consideration of our manuscript, and we look forward to a favorable decision.

Thank you and best regards.

Yours sincerely,

Prof. Hao Liang

State Key Laboratory of Chemical Resource Engineering, Beijing University of Chemical Technology, Beisanhuan Donglu 15 Hao, Beijing, P. R. China

Tel.: +86 10 64431557; Fax: +86 10 64437610.

E-mail address: lianghao@mail.buct.edu.cn

Designing biocompatible protein nanoparticles for improving the cellular uptake and antioxidation activity of Tetrahydrocurcumin.

Shan Chen [a], Qiao Wu [a], Mengyan, Ma [a], Zezhong, Huang [a], Frank Vriesekoop [c, *], and Hao Liang [a, b,*]

[a] *State Key Laboratory of Chemical Resource Engineering, Beijing University of Chemical Technology, Beijing 100029, P. R. China*

[b] *Qinhuangdao Bohai Biological Research Institute of Beijing University of Chemical Technology,Qinhuangdao 066000, China*

[c] *Department of Food Technology and Innovation, Harper Adams University, Newport TF10 8NB, Shropshire, England*

Corresponding Author

* E-mail: lianghao@mail.buct.edu.cn (Hao Liang);

FVriesekoop@harper-adams.ac.uk (Frank Vriesekoop)

Abstract:

Tetrahydrocurcumin (THC) is a natural molecule with anticancerous, antioxidant and other beneficial activities. However, its low aqueous solubility leads to poor bioavailability. Sodium caseinate (NaCas) is an ideal natural protein carrier with amphiphilic and non-toxic properties, which provides a new possibility for improving the aqueous solubility of THC. In this study, THC loaded protein nanoparticles (THC@NaCas) were successfully prepared by a nanoprecipitation method. The protein-based carrier awarded an encapsulation efficiency of about 98 % for THC. The structure and physicochemical characteristics of THC@NaCas nanoparticles were characterized by Fourier Transform Infrared Spectroscopy (FTIR), X-ray diffraction, and Scanning Electron Microscopy (SEM). The solubility test comfirmed that protein nanoparticles awarded greater solubility of THC. Furthermore, THC@NaCas had a greater antioxidant activity compared to free THC, resulting in a free radical scavenging ability of THC@NaCas 2.6 times greater than that of free THC. The *in vitro* cytotoxicity test showed that the THC@NaCas nanoparticles had a stronger inhibitory effect on cancer cells compared with free THC, and good biocompatibility for non-cancerous cells. In a short, Our results demonstrate that protein-based nanoparticles have the potential to improve the bioactivity of hydrophobic drugs in clinical application.

35 Keywords: Sodium Caseinate; Tetrahydrocurcumin; Nanoparticles; Cellular uptake;
36 Antioxidant

37

38 **1. Introduction**

39 Oxidative stress, induced by free radicals produced through normal cellular metabolism, has
40 been suggested to be a factor contributing to the development of various diseases such as
41 diabetes, cancer, atherosclerosis and neurodegeneration, and the accelerated onset of aging [1-3].
42 Free radicals, which have a single unpaired electron in their outer orbit, are able to damage and
43 alter a range of biomolecules including lipids, nucleic acids, and proteins in the body,
44 potentially leading to the onset of the above mentioned disorders [3, 4]. Therefore, there is an
45 urgent need for a drug or natural ingredient to eliminate the excessive free radicals produced in
46 the body.

47 Various phytochemicals possess properties that have antioxidant, anti-inflammatory, and
48 anti-cancerous properties [5]. Tetrahydrocurcumin (THC), a major metabolite of curcumin, has
49 displayed the ability to prevent oxidative effects caused by various diseases and has been shown
50 to possess anti-cancerous properties [3]. THC exhibits a greater antioxidant activity *in vivo*
51 systems when compared with curcumin and has shown the potential to control free radicals by
52 protecting cells against oxidative stress by trapping free radicals produced during diabetes [6].

In a clinical study conducted on male diabetic Wistar rats, THC was found to have a positive impact on erythrocyte membrane bound enzymes by imposing an antioxidant defence [6]. Compared with curcumin, THC is significantly more potent under physiological conditions, has higher antioxidant activity, and induces a more effective tumor angiogenesis [7, 8]. However, THC has poor aqueous solubility, degrades rapidly on exposure to oxygen and is poorly absorbed in the gastrointestinal tract, which hinders its dietary/nutraceutical application [5, 9]. Hence the requirement for the development of a natural delivery system can overcome the disadvantages in the efficient delivery of THC.

It has been reported that the delivery of active drugs to the cytoplasm of tumor cells must go through five steps. (1) Nanoparticles are transported through the blood circulation. (2) The permeability of nanoparticles makes them accumulate in tumor site. (3) Gradually penetrate into tumor tissue. (4) Nanoparticles are internalized by tumor cells via endocytosis. (5) Active drug release via lysosome [10, 11]. Therefore, ideal drug delivery systems have a high drug loading efficiency and nanocarriers with large surface area to volume ratio which improve the delivery of the drug to the required tissues/cells [9]. The biocompatibility and efficiency of natural compounds, which are now considered key components in the prevention of diseases such as cancer, diabetes, and inflammation, are markedly improved through the creation of protein-based delivery systems [3]. In a protein-based drug delivery system, proteins are used

as stable encapsulation carriers with the ability to improve dispersion, protect the compounds they carry and improve the physical stability of these compounds in a range of environments [9, 12]. Sodium caseinate's amphiphilic tendencies makes it an effective protein used in drug delivery systems [13]. Sodium caseinate (NaCas), is derived from caseinate, a protein typically derived from bovine milk [14, 15]. NaCas is produced following the precipitation of casein at its isoelectric point (pH 4.6) and the readjustment of the pH to 6.7 using sodium hydroxide [16]. Due to its high content of hydrophobic amino acids, NaCas has emulsifying properties which makes it as a naturally occurring amphiphilic block copolymer [5, 13]. Amphiphilic block copolymers exhibit both immiscibility in water and hydration tendencies, properties that are necessary to encapsulate hydrophobic bioactive compounds such as THC [5, 17]. Amphiphilic block copolymers are commonly used for drug delivery systems, specifically as carriers for nanomedicine [18], which self-assemble in aqueous solutions to form micelles [17]. When the NaCas micelles self-assemble they can encase the hydrophobic bioactive compounds, the micelles then act as an effective carrier to improves the dispersibility of the encapsulated guest compounds in aqueous solution [17-20].

In this study, sodium caseinate was employed to encapsulate THC in a green and safe self-assembled manner to facilitate an enhanced cellular uptake and antioxidant activity (**Scheme 1**). The efficiency of THC incorporation into NaCas was assessed by means of Fourier

Transform Infrared (FTIR) spectroscopy and X-Ray Diffraction (XRD), following which the encapsulated THC was evaluated for its antioxidant capabilities and cell uptake through testing on non-cancerous embryonic cells (3T3 cells) and cancerous melanoma cell (A375 cells). Our results showed that the cell uptake and antioxidant capabilities of THC were significantly improved and the prepared nanoparticles had good biocompatibility.

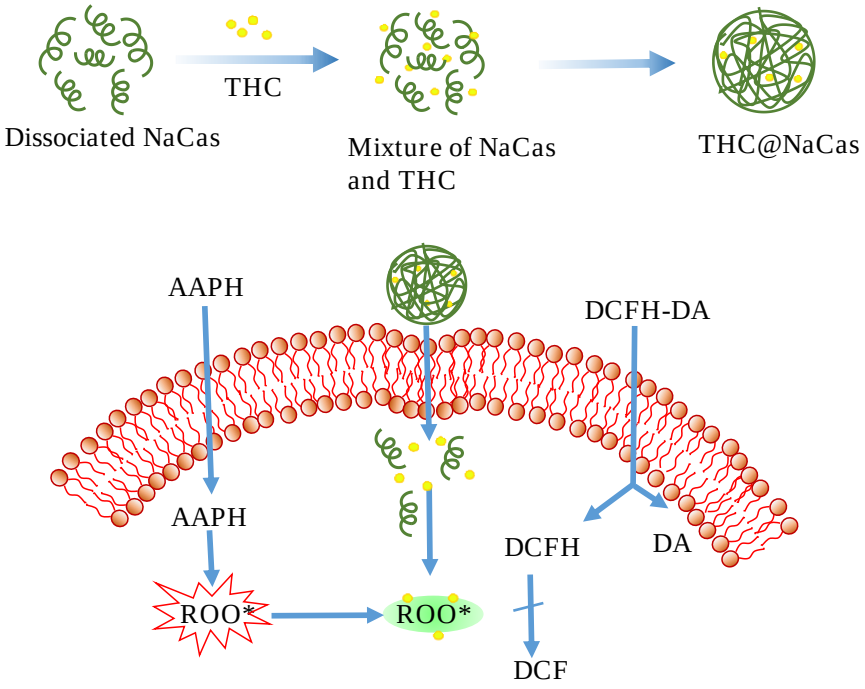

Scheme 1: Schematic representation of the synthesis, cellular uptake and cellular antioxidant activity of THC@NaCas. After the DCFH-DA entered the cells, it cleaved into DA and DCFH, AAPH decomposed and produced free radicals, which could transform DCFH into fluorescent DCF, THC@NaCas were able to scavenge the free radicals to reducing the production of DCF.

2. Materials and methods

2.1. Materials

2,2-Azobis(2-amidinopropane)-dihydrochloride (AAPH) and 2,7-dichlorodi-hydro-fluorescein diacetate (DCFH-DA) were obtained from Sigma-Aldrich (St. Louis, MO, USA). Sodium caseinate (NaCas) and tetrahydrocurcumin (THC) were purchased from Mackin Biochemical (Shanghai, China). L-tyrosine (25KU, from mushroom) was supplied by Aladdin Inc. (Shanghai, China). Dimethyl sulfoxide (DMSO) was bought from Sinopharm Chemical Reagent Co., Ltd (Shanghai, China). Cell Counting Kit-8 (CCK-8) was purchased from Dojindo Laboratories (Tokyo, Japan). 3T3 cells (Mouse embryonic fibroblasts) and A375 cells (Human melanoma cells) were got from the Cell Resource Center, Peking Union Medical College (Beinjing, China). The cell culture medium was DMEM with 10 % Fetal Bovine Serum, and the cells were incubation with 5 % CO_2 and 95 % air at 37 ºC. All other materials were obtained from Beijing Biochemical (Beijing, China).

2.2. Synthesis of THC@NaCas

The THC stock solution was prepared by dissolving 20 mg of THC in 10 mL ethyl alcohol. The NaCas stock solution was prepared by dissolving 200 mg of NaCas in 100 mL deionized water under vigorous stirring for 30 minutes. To create the THC@NaCas, 10 mL of THC

solution was dropwise added into 100 mL of NaCas solution under vigorous stirring for 4 hours at room temperature. Then the mixed solution was centrifuged at 400 g for 10 minutes. The supernatant contained THC@NaCas and the precipitation was THC which had not been successfully encapsulation. Followed, the un-encapsulated THC was measured using UV-visible spectrophotometer (Shimadzu, UV-2450, Japan) at 280nm in order to evaluate the encapsulation efficiency (EE). Then the supernatant was freeze-dried to obtain solid powder and used to determine THC loading capacity (LC). The LC of THC was tested by high performance liquid chromatography (HPLC) (LC-15C, Japan) with a detection wavelength is 280 nm. Acetonitrile and phosphoric acid aqueous solution (50:50, v/v) were used as a mobile phase. Ethanol was used to extract the encapsulated THC from the protein nanoparticles, and then the ethanol solution was filtered by 0.22 μm membrane to remove the insoluble protein. The EE and LC were calculated according to the following equations:

$$\text{EE}\ (\%) = \frac{total\ amount\ of\ added\ THC - amount\ of\ THC\ on\ the\ bottom}{total\ amount\ of\ added\ THC} \times 100\%$$

$$\text{LC}\ (\%) = \frac{\text{amount of THC loaded}}{total\ amount\ of\ NPs} \times 100\%$$

2.3. Characterization of THC@NaCas

The particle size and zeta potential of NaCas and THC@NaCas were measured using a

dynamic light scattering instrument at 25 ºC (Mastersizer 2000, Malvern Instruments Ltd., Malvern, Worcestershire, UK). Before the measurement, a certain amount of solid powder was diluted with deionized water. Each set of data was collected by balancing the emulsion in the measuring room for 120 s.

The morphology of NaCas and THC@NaCas was recorded using a HITACHI S-4700 scanning electron microscope (SEM) (Tokyo, Japan). All samples were attached to brass stubs with double-sided tape before sputtered-coated with a thin gold layer for analysis.

The X-ray diffraction patterns of THC, NaCas and THC@NaCas were recorded on an X-ray diffractometer (Bruker, D8 ADVANCE, Karlsruhe, Germany) equipped with a copper target X-ray tube. The voltage and current applied were set at 40 kV and 40 mA, respectively. The diffraction angles were scanned from 5° to 90° in 2θ at a scan rate of 10°/min and a step of 0.02°.

A FTIR spectrometer (JASCO FT-IR 6600, Madison, WI, USA) equipped with a DLaTGS detector was used to investigate the changes in the secondary structure of the NaCas as well as the dynamics of its interaction with THC. THC, NaCas and THC@NaCas were pressed into KBr salt tablets at 10 mg sample per g of KBr with the spectrometric scanning range between 4000 and 400 cm^{-1}.

In order to determine the effect of temperature and concentration on the solubility of

154 THC@NaCas in water, various amounts of THC@NaCas powder were dissolved in 20 mL
155 deionized water. The final concentrations of THC@NaCas suspensions were 0, 10, 20, 30, 40,
156 50 mg/mL. The THC@NaCas suspensions were agitated in an orbital shaking incubator at 100
157 rpm for 30 min at either 25 °C or 37 °C, following which samples were filtered through a 0.22
158 μm membrane to remove any insoluble substances. 500 μL of the filtrate was taken and diluted
159 with absolute ethanol to 12.5 mL. The absorbance was measured at 280 nm UV-visible
160 spectrophotometer (Shimadzu, UV-2450, Japan) and the THC dissolution was calculated
161 compared with the standard curve ranging from 6 to 14 μg/mL THC which had a correlation
162 coefficient of R^2>0.994 (Figure S1).
163
164 ***2.4. Stability evaluation of THC@NaCas***
165 Thermal stability and pH stability of free THC and THC@NaCas were determined according
166 to previous research methods [21, 22] with appropriate modification. Two solutions containing
167 the same amount of THC were placed at 80 ºC water bath and heated continuously for several
168 hours. Taking out a certain volume of liquid every half an hour and detecting THC content by
169 high performance liquid chromatography (HPLC). Similarly, a certain amount of THC@NaCas
170 solid powder and free THC were dissolved into different phosphate buffer solution respectively
171 (pH=7.0 and pH=5.4) for 2 hours. Finally, the retention rate was selected as the index to reflect

the stability of THC, the initial concentration of THC in all samples was set as 100 %.

2.5. In vitro release of THC@NaCas

The *in vitro* release kinetics of THC@NaCas in stimulated gastric fluid and normal saline were studied according to previous method [23] with appropriate modification. First, 50 mg THC@NaCas freeze-dried powder was dissolved in deionized water and dispersed in dialysis bag (MWCO, 3500Da). The dialysis bag was soaked in 200 mL stimulated gastric fluid (SGF, 2.0 mg/mL NaCl, 3.8 mg/mL pepsin and hydrochloric acid adjusts pH to 1.2) or saline solution (pH=7.0) and was stirred slowly at the speed of 100 rpm under 37 ºC. A certain time interval, 1 mL solution was extracted and added the same volume of fresh solution.

2.6. Cellular uptake of THC@NaCas

The intracellular delivery of THC@NaCas was evaluated by Confocal Laser Scanning Microscope. Cultured human melanoma cells (A375 cells) were allowed to attach to the surface of the laser confocal dish for 12 h. Then the cells were treated with equal concentration of free THC or THC@NaCas (2 mL, 5 μg/mL) for 6 h, after which the cells were washed using fresh PBS and then fixed by adding a 4% paraformaldehyde solution. Finally, the cells were stained by adding 200 μL the nucleus-staining 4,6-diamidino-2-phenylindole (DAPI) dye for 15 min.

190 The confocal laser scanning microscope images were obtained by exciting THC and DAPI at
191 405 nm, with emissions measured at 410 nm and 460 nm respectively.
192
193 ***2.7. Cell toxicity test***

194 The relative toxicity of free THC and THC@NaCas were tested on non-cancerous mouse
195 embryonic cells (3T3 cells) and cancerous human melanoma cells (A375 cells) according to a
196 modified CCK-8 method described elsewhere [24]. Both cell types were inoculated at a density
197 of 6×10^4 cell/well in 96-well microplates and incubated at 37 °C for 24 h, containing 50 µL of
198 cell suspension and 50 µL different concentrations of THC (at 0, 1, 2, 3, 4, 5 µg/mL) and
199 THC@NaCas (also at 0, 1, 2, 3, 4, 5 µg THC-equivalent/mL). Progression in cell growth was
200 determined by measuring the optical density 450 nm by UV-VIS spectrophotometer. Three
201 independent experiments were run with nearly identical results. The cell survival rate was
202 calculated according to the following equations:

203 $$\text{Cell survival rate}(\%) = \frac{\text{Abs } treatment}{\text{Abs } blank} \times 100\%$$

204
205 ***2.8. Cell antioxidant capacity test***

206 The cellular antioxidant activity (CAA) of THC@NaCas was determined by the CAA
207 method according to Wolf and Liu [25] and modified appropriately. Both cell types (3T3 cells

and A375 cells) were seeded at a density of 6×10^4 cell/well on 96-well microplates (100 μL per well). Each sample was treated with 10 μL of THC or THC@NaCas solution at various concentrations, plus 5 μL of 2′,7′-dichlorodihydrofluorescein diacetate (DCFH-DA) (25 μM). After incubation at 37 ºC for one hour, each sample was treated with 2,2′-azobis (2-amidinopropane) dihydrochloride (AAPH) (1.2 mM, 100 μL). Samples were then incubated for one hour at 37 °C with the fluorescence being measured every 5 min at the excitation wavelength of 538 nm and the emission wavelength of 485 nm [25]. Following this, the quantification of CAA was undertaken according to Wolfe and Lui [25] using the following equation:

$$\mathrm{CAA(unit)} = 100 - \frac{\int \mathrm{SA}}{\int \mathrm{CA}} \times 100$$

Where ∫ SA represents the integrated area under sample time-fluorescence curve; while ∫ CA represents the integrated area from control curve.

2.9. Tyrosinase inhibition experiment

THC is a known inhibitor of tyronase [26], as such we investigated the inhibitory influence of both free and encapsulated THC on tyrosinase activity. The THC@NaCas nanoparticles were prepared by mixing 1mL of NaCas (2.0 mg/mL) with 100 μL of THC (2.0 mg/mL), which was vigorously stirred by means of a magnetic stirrer for 30 min. From this stock solution four

226 THC@NaCas nanoparticles samples were diluted with PBS to different concentrations of THC
227 (5, 10, 15 and 20 μg /mL), while free THC was diluted with PBS to the same concentration as
228 the THC@NaCas nanoparticles. The different nanoparticles of THC@NaCas and free THC
229 were mixed with 0.5 mL of L-tyrosine and kept at 37 °C for 5 min. Then 0.25 mL of tyrosinase
230 (100 Units/mL) in PBS and 1.25 mL of PBS were added into each solution and incubated at
231 37 °C for 10 min with continuous agitation, following which the absorbance was measured at
232 475 nm [27]. Determining the inhibition of tyrosinase activity was based on the following
233 equation [26, 28].

234 $$Inhibition = \frac{A - B}{A} \times 100\%$$

235 A represents the absorbance of the sample, B represents the absorbance of the blank control.

236

237 **3. Results and discussion**

238 ***3.1. Preparation and characterization of THC@NaCas***

239 In order to maximize the content of THC in prepared nanoparticles, we studied the influence
240 of different concentrations of THC on the LC and EE. **Table 1** showed the LC and EE of THC
241 by using different ratio of NaCas and free THC. When the concentration of NaCas was 1
242 mg/mL, the LC of THC was gradually increased from 2.30 % to 2.76 % as the increase of the
243 concentration of THC solution. The EE of THC increased to a certain value and then began to

decline. Similar results were found at the concentration of NaCas was 2 mg/mL. When the concentrations of NaCas and THC were both 2mg/mL, it had the best LC (3.00 ± 0.26 %). We chose the condition to prepare THC@NaCas in the following research.

The surface potential and the average diameter of nanoparticles were also characterized by dynamic light scattering (DLS). The surface potential of THC@NaCas increased slightly compared with NaCas, which increased from -22.5 mV to -21.3 mV (**Table. S1**). The high surface negative potential endows THC@NaCas with high stability and good dispersion as a result of electrostatic repulsion between the particles. The particle sizes of NaCas and THC@NaCas were 263.6 nm and 269.8 nm, respectively. This result indicated that THC successfully inserted into the hydrophobic site of NaCas, so that the nanocomposite still maintain a small size.

SEM was applied to visualize the surface morphology of NaCas and THC@NaCas particles (**Fig**. **1A** and **Fig. 1B**). The morphology of NaCas was relatively uniform and spherical (Fig. 1A), which was consistent with previous reports [29]. Following the encapsulation of THC in NaCas the morphology of the THC@NaCas changed not only in shape but also in size, which agreed with the results of previously reported encapsulating experiments [30]. The morphology of the THC@NaCas showed uneven and irregular spherical and angular shapes (**Fig. 1B**). This was taken as an indication that THC was encapsulated into a NaCas casing.

X-ray diffraction (XRD) was applied to investigate the nanoparticle formation of THC encapsulation into NaCas (**Fig. 1C**). Our results revealed that pure THC displayed obvious and characteristic peaks at angles 8.16, 11.48, 14.40, 17.78, 24.02, which was consistent with a previous report [31], indicating that pure THC was in a highly crystalline form. However, no obvious peaks were detected in the XRD patterns of NaCas, displaying amorphous characteristics. The THC@NaCas scan displayed a more amorphous background with only some minor evidence of crystalline forms. The minor crystalline signals might be due to fractions of the entrapped THC protruding from the NaCas casing, which was likely to be the result of the spontaneous encapsulation of free THC by NaCas, as also described elsewhere [32]. However, the self-assembly that occurred when the THC@NaCas was formed proved that the spontaneous encapsulation shielded most of the crystalline THC from the external environment. The crystalline peaks that were observed for THC@NaCas did not line up entirely with the peak seen for pure THC, the most likely explanation for this was that the presence of the caseinate proteins caused some steric hindrance during crystal packing affecting its configurative alignment [33].

We further investigated the nanoparticle formation of the encapsulation of THC by NaCas by means of FTIR spectroscopy (**Fig. 1D**). Our results revealed changes in the secondary structure of NaCas as well as the dynamics of its interaction with THC. THC was characterized by

distinct absorption peaks at 3417 cm^{-1} and 2848 cm^{-1} (O-H stretching on the phenolic groups), 1720 cm^{-1} (C=O stretching on the diketone groups), 1614 cm^{-1}, 1000 cm^{-1} and 700 cm^{-1} (C=C bending on the aromatic rings), 1515 cm^{-1} (C=C stretching in aromatic ring), 1450 cm^{-1} (C-H bending on methyl groups) and 867 cm^{-1} (C-H bending on alkane chains), and 1300-1200 cm^{-1} (=C-O-CH_3 stretching of alkyl-aryl ether groups) [34].

NaCas was characterized by broad absorption peaks between 3500 and 2700 cm^{-1}, which included N-H stretching due to the secondary amines in the peptide bonds and C-H stretching on the peptides and a distinct peak near 3100 cm^{-1} due to amine salts, the peak position of the amide-I band of NaCas at 1740 to 1680 cm^{-1} (C=O stretching, representing an α-helix structure), and its amide-II was occurred at 1640 cm^{-1} (C-N stretching coupled with N-H bending, representing antiparallel β-sheet structures), 1520 cm^{-1} (-CH_2 shear vibration), and 1200 cm^{-1} (C-O bending) [35].

The FTIR spectrum of the THC@NaCas was broadly similar to NaCas over the range from 4000 to 2000 cm^{-1}, which represented the principle peptide related absorbances. After NaCas encapsulated THC, the peak position of NaCas for the amide-I band shifted from 1739 cm^{-1} to 1652 cm^{-1} and for the amide-II band from 1640 cm^{-1} to 1519 cm^{-1}, indicating a conformational change in the NaCas peptides due to the steric effect of THC on NaCas. Similarly, the peaks for the alkyl-aryl ether groups on THC appeared to have shifted from 1300-1200 cm^{-1} to 1100-1000

298 cm^{-1}, which reiterated the XRD results that the presence of the caseinate proteins influence the
299 molecular packing of encapsulated molecules, affecting their configurative alignment. These
300 results indicate that the formation of nanocomposites between NaCas and THC was
301 accompanied by changes in secondary structure and chemical microenvironment of both NaCas
302 and THC.

303 In order to assess whether THC has a greater overall solubility when encapsulated into
304 NaCas compared to free THC we dissolved both free THC and THC@NaCas into deionized
305 water at two different temperatures. In the subsequent phase solubility experiments (**Fig. S2**),
306 we found that the solubility of THC incorporated as THC@NaCas increased with the increase
307 of concentration at both 25 °C and 37 °C, with a greater solubility at 37 °C compared to 25 °C.
308 The solubility of THC in deionized water was calculated to be 258.3 µg/mL and 179.2 µg/mL at
309 37 °C and 25 °C respectively when the concentration of THC@NaCas suspensions were 10
310 mg/mL. The solubility of THC in THC@NaCas was 53 and 28 times higher compared to free
311 THC (3.4 µg/mL at 25 °C and 9.2 µg/mL at 37 °C). Hence, the solubility is markedly improved
312 when encapsulated into a NaCas casing, which is in agreement with findings by Park and
313 coworkers who reported similar results when encapsulating turmeric into a biodegradable
314 carrier [36].

315 **Table 1**

The loading capacity and encapsulation efficiency of THC on different condition

NaCas (mg/mL)	THC (mg/mL)	EE (%) ± SD	LC (%) ± SD
1	0.5	86.64 ± 0.67	2.30 ± 0.08
1	1	95.95 ± 0.49	2.45 ± 0.12
1	1.5	94.91 ± 0.58	2.56 ± 0.25
1	2	87.36 ± 0.89	2.76 ± 0.17
2	0.5	97.60 ± 0.73	2.47 ± 0.39
2	1	98.63 ± 1.23	2.63 ± 0.34
2	1.5	98.71 ± 0.66	2.71 ± 0.09
2	2	96.34 ± 0.23	3.00 ± 0.26

Abbreviation: NaCas: sodium caseinate; THC: Tetrahydrocurcumin; EE (%): encapsulation efficiency; LC (%): loading capacity. All measurements are means ±SD (n=3).

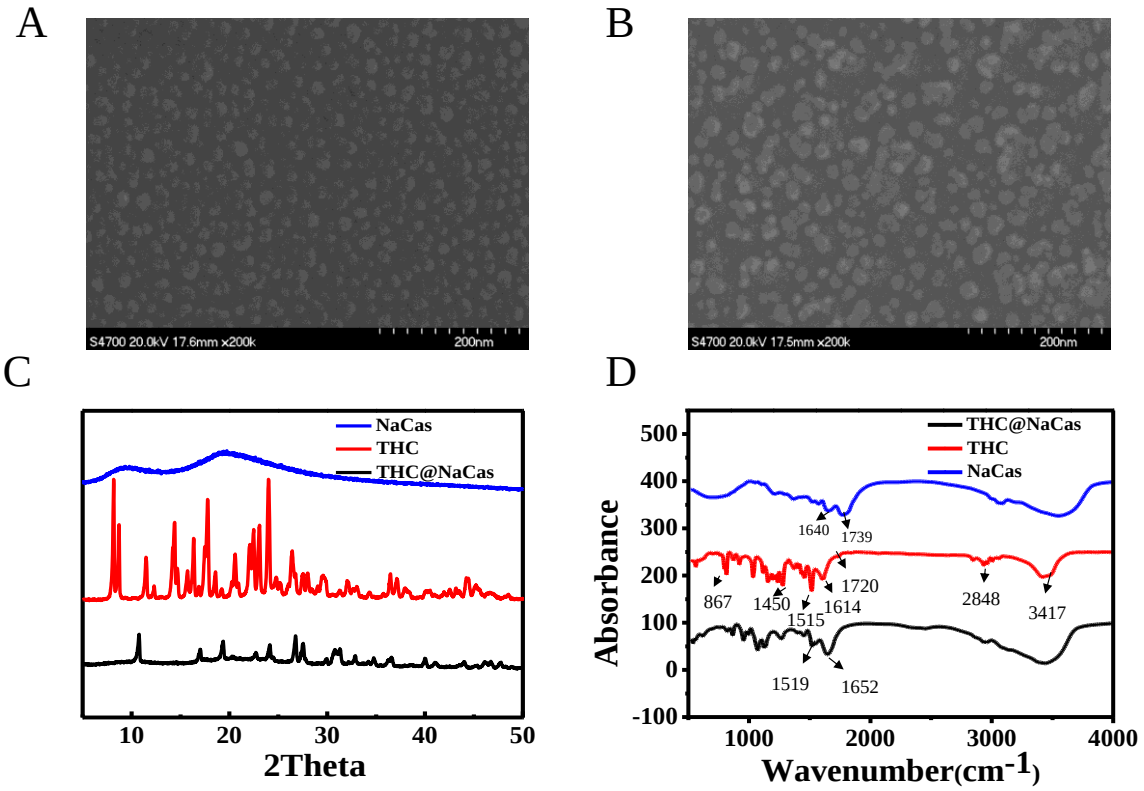

321

322 **Fig. 1**. Characterizations of nanoparticles. SEM images of (A) NaCas and (B) THC@NaCas. (C)

323 XRD spectra and (D) FTIR analysis of NaCas, THC and THC@NaCas.

324

325 ***3.2. Stability of THC@NaCas***

326 The stability of free and encapsulated THC in extreme environments was also studied, such

327 as high temperature and strong acidic conditions. Thermal stability experiment (**Fig. 3A**)

328 showed that free THC had good thermal stability. After heated at 80 ºC for 2.5 h, the

329 degradation rate of free THC was only 20 %. THC was encapsulated with NaCas not only had

330 no effect on the stability but further improvement. Free THC and THC@NaCas also could

331 maintain strong stability in different pH solution. As shown in **Fig. 3B**, THC@NaCas degraded

more slowly in phosphate buffer solution of 7.0 compared to 5.4. The instability of NaCas in acidic conditions led to the degradation rate of THC@NaCas faster than in neutral environment.

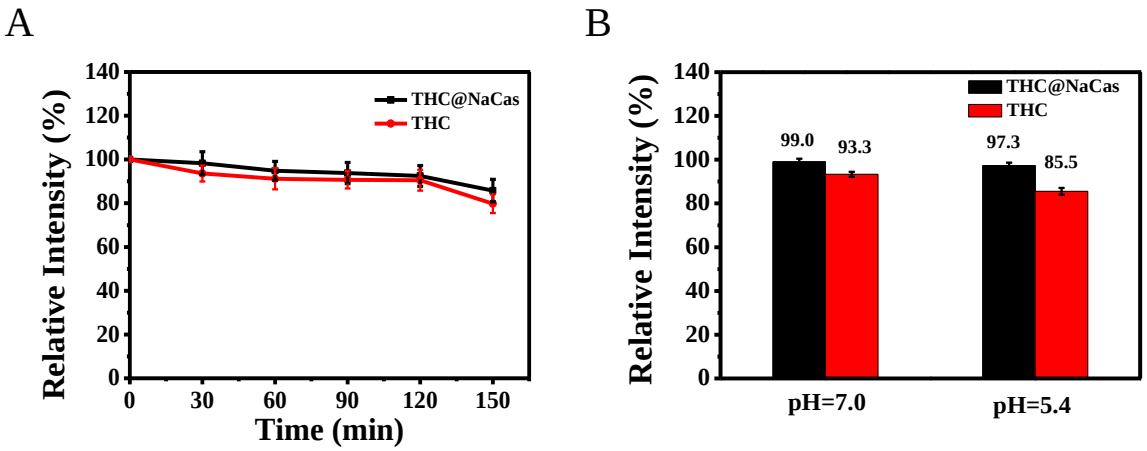

Fig. 3. The stability of free THC and THC@NaCas at 80 ℃ and different pH. (A) The degradation curve of free THC and THC@NaCas at 80 ℃. (B) Retention of free THC and THC@NaCas after storage in different phosphate buffer solution (PBS) for 2 hours.

3.3. In vitro release of THC@NaCas

In order to study the release kinetics of THC from THC@NaCas in stimulate gastric fluid and normal saline, we dispersed THC@NaCas in two solutions at the same time. As shown in **Fig. 4,** the release of THC from THC@NaCas was faster in acidic gastric fluid than in normal saline. In the first 2 hours, the release of THC showed a rapid trend, the release of THC reached 45 % in stimulate gastric fluid and 40.2 % in normal saline. This might be due to some weak absorptive THC existed near the surface of sodium caseinate. Similar experimental phenomena

had also been reported in past study [37]. Subsequently, THC released more slowly and presented a slower and more lasting release pattern. The above phenomena indicated that NaCas could effectively restrain THC release from THC@NaCas. This will greatly prolong the residence time of THC in clinical application and keep lasting pharmacodynamics activity.

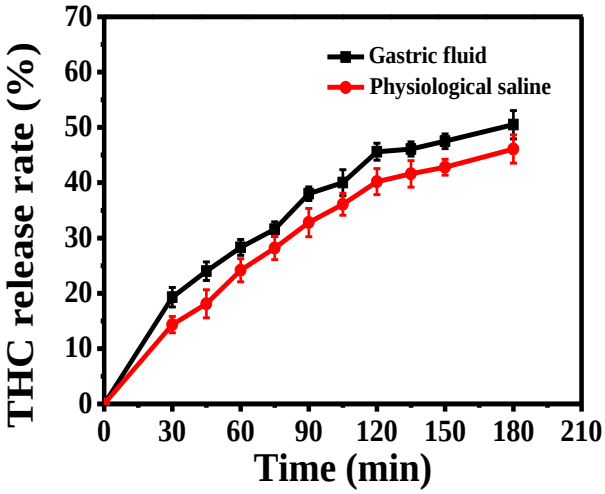

Fig. 4. The release kinetic curve of nanoparticles in stimulate gastric fluid and normal saline.

3.4. Cellular uptake of THC@NaCas

Cellular uptake capacity is an important factor for evaluating the intracellular biological activity of drugs [38]. Thus, we used confocal laser scanning microscope (CLSM) to observe the delivery of THC@NaCas in cancerous human melanoma (A375) cells. The cells were co-cultured separately with THC and THC@NaCas, while in the control group the cells were co-cultured with DMSO. The blue fluorescence visualizes the structure of A375 cells and the green fluorescence visualizes the intracellular distribution of THC in the cells. At equal

concentrations of THC, both free THC and THC@NaCas were co-cultured with A375 cells (**Fig. 5**). Encapsulated THC (THC@NaCas) showed a much more pronounced fluorescence compared to free THC, suggesting that the ability of THC to enter cells was enhanced through forming THC@NaCas. Furthermore, the rapid degradation of free THC in cancer cells could also have led to a weak fluorescence signal. Our results showed that encapsulated THC (THC@NaCas) could facilitate the stability of THC and release THC into the intracellular environment of cancer cells.

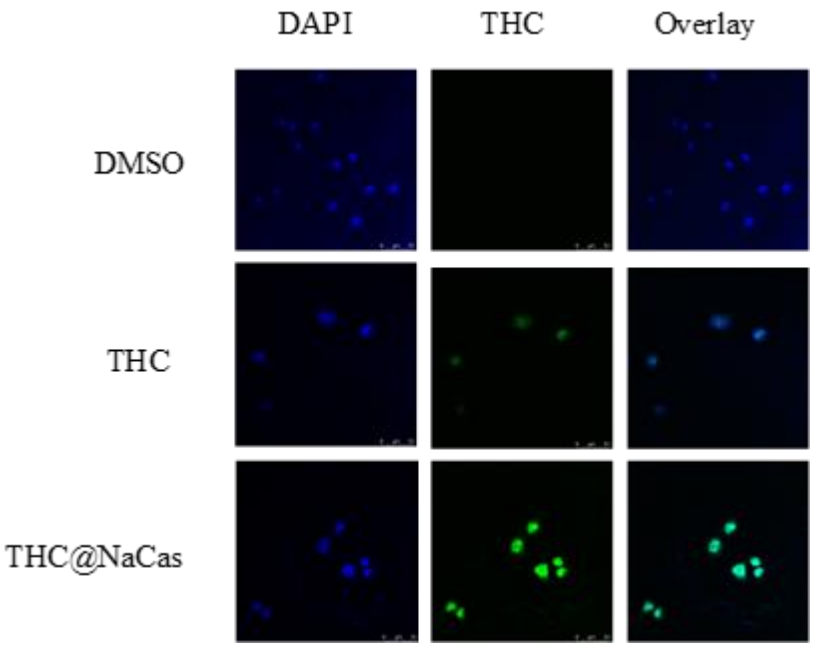

Fig. 5. Confocal laser scanning microscopy images of cancerous human melanoma (A375) cells after incubation with DMSO, THC and THC@NaCas for 4 h. (Nanoparticles: 2 μg/mL; DAPI: cell nuclear blue fluorescent probe).

3.5. Cell toxicity test

To determine the effects of THC on the survival/viability of cancerous and non-cancerous cells, in a free form and the encapsulated form (NaCas), we applied the CCK-8 assay [24]. The non-cancerous mouse embryonic cells, were not negatively affected by the presence of either free or encapsulated THC under the conditions of our experiment (**Fig. 6A**). These results suggested that THC had good biocompatibility with healthy non-melanoma cells and displayed no biological toxicity. Furthermore, THC@NaCas appeared to promote the growth of mouse embryonic cells at the lowest concentration (cell survival reached 123 % at 1 µg/mL), but the growth-stimulation effect did not persist at any of the higher THC@NaCas concentrations (c > 2 µg/mL). Free THC imposed a growth-stimulation effect on the non-cancerous mouse embryonic cells at almost all concentrations tested with an average growth stimulation at 111.2 ± 8.3% (**Fig. 6A**). This stimulatory effect might be due to the upregulation of the FOXO4 transcription factor by THC, which had been shown to linked to longevity in 3T3 cells [39].

Free THC did not inhibit the growth of cancerous human malignant melanoma cells at low concentrations, in fact growth was somewhat stimulated at concentrations up to 3 µg/ml (**Fig. 6B**). However, the growth of the malignant melanoma cells was retarded at the higher concentrations (cell viability was 95 % and 91 % at 4 and 5 µg/mL respectively). THC@NaCas

imposed an inhibitory effect on growth at almost all concentrations (**Fig. 6B**), with a very marked growth inhibition at 4 and 5 μg/mL and the cell viability was 94 % and 87 % respectively. Similar results with curcumin rather than THC were shown elsewhere [40-42], Several studies suggested that curcumin induced A375 cells apoptosis by modulating multiple signaling pathways to exert its anticancer effect and caused DNA damage in A375 cell [43, 44]. THC inhibited the growth of mouse hepatoma cells (H22 cells) by inducing mitochondrial apoptosis in previous study [45]. At present, there is no related literature report on the anticancer mechanism of THC against A375 cells.

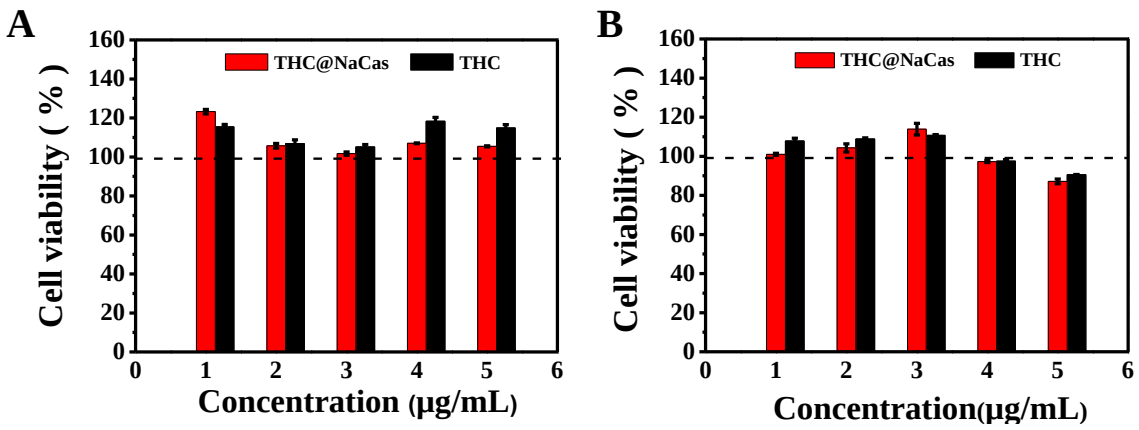

Fig. 6. Cell toxicity of THC and the THC@NaCas against mammalian cell lines at different concentrations. (A) Cell toxicity against non-cancerous mouse embryonic (3T3) cells. (B) Cell toxicity against cancerous human melanoma (A375) cells.

3.6. Cell antioxidant capacity test

To further investigate the antioxidant capabilities of THC and THC@NaCas, we adapted the

405 cellular antioxidant capacity (CAA) assay as described by Wolf and Liu [25]. The free radical
406 scavenging ability of THC can be reflected by monitoring the fluorescence intensity caused by
407 dichlorofluorescein (DCF). The principle of CAA was showed in **Scheme 1**. Mouse embryonic
408 cells (normal cells) and malignant human melanoma cells (tumor cells) were chosen as models
409 to evaluate intracellular antioxidant capacities. Our data revealed that in both cells
410 THC@NaCas had a greater ability to scavenge free radical compared to free THC (**Fig. 7A**
411 **&C**). When calculating the corresponding CAA units, it was found that the free radical
412 scavenging capacity of THC@NaCas in non-cancerous mouse embryonic cells and cancerous
413 human melanoma cells reached 29.15 and 12.58 respectively, which was 1.84 and 2.56 times of
414 the response of free THC (**Fig. 7B &D**). The elevated CAA response due to the presence of
415 THC@NaCas indicates the greater ease by which THC can be delivered into the cells,
416 regardless of whether they are cancerous cells or not. However, the reduced CAA response
417 when comparing cancerous and non-cancerous cells (regardless of whether the THC was
418 encapsulated) reiterates the possibility that THC has the ability to reduce the effective ability of
419 glutathione by depleting it [46]. Antioxidants like THC play an important role in the protection
420 against oxidative stress, especially in the case of cancer [37], more specifically THC has been
421 shown to cause a decrease in gene expression leading to anti-angiogenesis [47]. As mentioned
422 before, it appears that cancerous cells must have a greater inherent requirement for glutathione

and that even at relatively low concentrations of THC their viability is reduced.

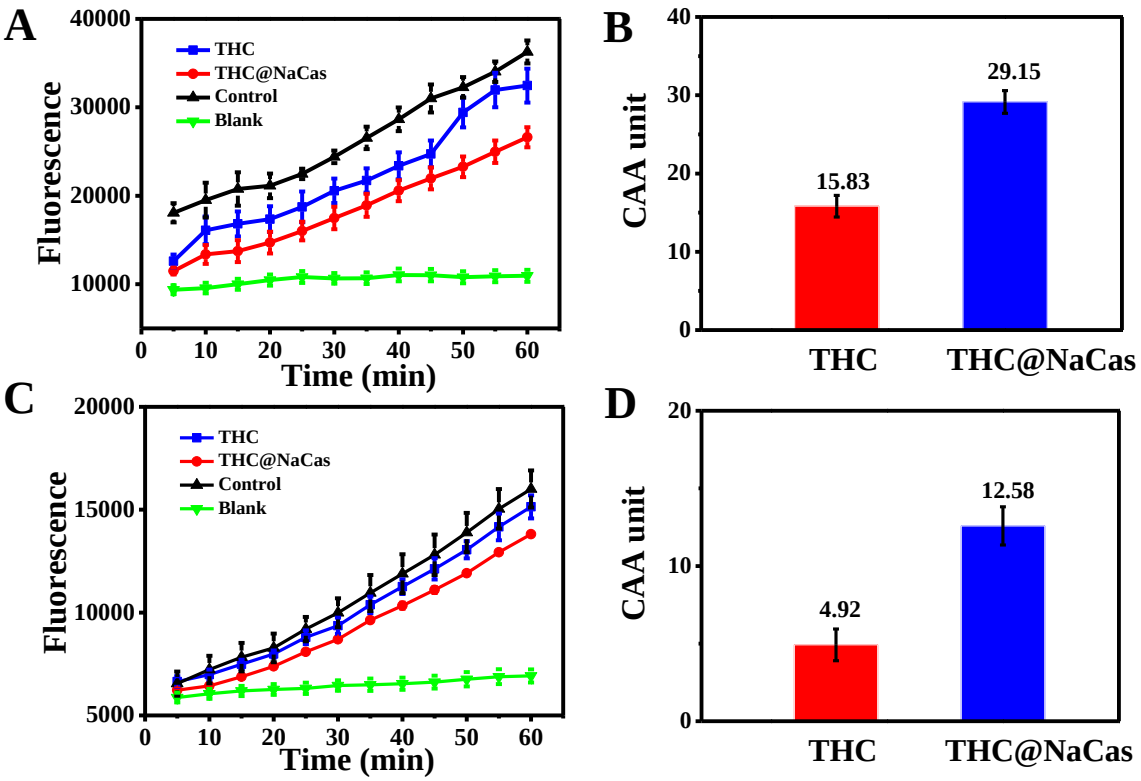

Fig. 7. The cellular antioxidant capacity of THC and the THC@NaCas. (A) Kinetics curve of DCF fluorescence from CAA of THC, THC@NaCas, control and blank sample against non-cancerous mouse embryonic (3T3) cells. (B) CAA values of THC and THC@NaCas against non-cancerous mouse embryonic (3T3) cells. (C) Kinetics curve of DCF fluorescence from CAA of THC, THC@NaCas, control and blank sample against cancerous human melanoma (A375) cells. (D) CAA values of THC and THC@NaCas against cancerous human melanoma (A375) cells.

3.7. Tyrosinase inhibition by free and encapsulated THC

THC is a known inhibitor of tyronase [26], an enzyme involved in the proliferative production of melanin. The inhibitory influence of both THC and THC@NaCas on tyrosinase was tested *in vitro*. The inhibitory effect of both free THC and THC@NaCas increased with the increase of the total concentration of THC (**Fig. 8**), however the inhibitory effect of encapsulated THC (THC@NaCas) was more pronounced compared to free THC. When the concentration of THC is 10 µg/mL, the inhibition effect of THC@NaCas is about 20 times more potent compared to free THC. Similarly, the tyronase inhibitory effect of 10 µg/mL THC as THC@NaCas was similar to the tyronase inhibitory effect at 20 µg/mL of free THC, indicating that the ultimate dose of THC could be halved if encapsulated to achieve the same inhibitory results. These results indicate that the bioavailability of encapsulated THC is markedly improved at low THC concentrations. This high tyrosinase inhibition activity might be attributed to the good dispersion and stability of encapsulated THC nanoparticles in an aqueous solution.

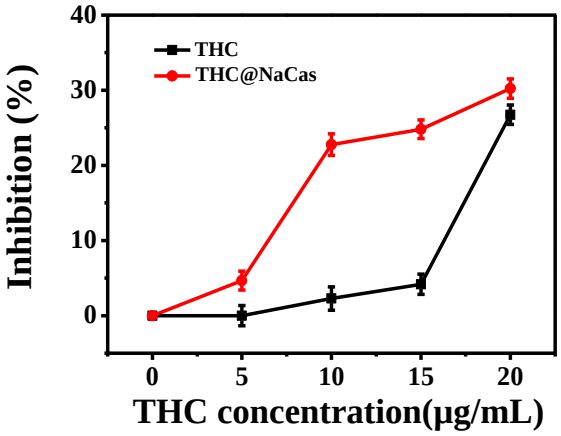

Fig. 8. The inhibition activity of THC and THC@NaCas on tyrosinase at different THC concentration

4. Conclution

In this study, THC was successfully encapsulated in sodium caseinate to form THC@NaCas nanoparticles. FTIR and XRD analyses demonstrated the THC@NaCas particles were formed efficiently with the THC entrapped within a conglomerate protein matrix. The encapsulation of THC in NaCas greatly improved the antioxidant activity, the cellular uptake and the inhibition activity on tyrosinase of THC. Besides, the *in vitro* cytotoxicity test showed that the THC@NaCas nanoparticles had inhibitory effect on cancer cells, however no inhibitory effects were observed against non-cancerous cells by either free THC or THC@NaCas. Therefore, in terms of clinical application perspective, THC@NaCas can be used as a safe and effective anti-melanoma drug for medical treatment. In addition, it can also be used as an additive in

cosmetics, which has good antioxidant effects and have no any toxic effect on other tissues of the human body. It can be seen from our experimental results that NaCas has a strong advantage as a carrier of nano-delivery system. It can not only improve solubility and stability of hydrophobic drugs but also delay the release of drugs. Cell uptake result also shows that NaCas can enhance the cellular uptake of hydrophobic drugs. All in all, NaCas is a viable and promising candidate for the safe and effective encapsulation of THC to improve its bioavailability in clinical treatment.

Notes

The authors declare no competing financial interest.

Acknowledgements

The authors acknowledged financial support from Hebei Key Research and Development Project (20372508D) and National Natural Science Foundation of China (21878014 and 22078014).

Appendix A. Supplementary data

Supplementary data to this article can be found online.

480 **Refernces**

481 [1] H.N. Sun, Y. Liu, X. Bai, X.F. Zhou, H.Y. Zhou, S.J. Liu, B. Yan, Induction of oxidative
482 stress and sensitization of cancer cells to paclitaxel by gold nanoparticles with different charge
483 densities and hydrophobicities, J Mater Chem B 6(11) (2018) 1633-1639.

484 [2] P. Murugan, L. Pari, Antioxidant effect of tetrahydrocurcumin in
485 streptozotocin-nicotinamide induced diabetic rat, Life Sci 79(18) (2006) 1720-1728.

486 [3] J.C. Wu, M.L. Tsai, C.S. Lai, Y.J. Wang, C.T. Ho, M.H. Pan, Chemopreventative effects of
487 tetrahydrocurcumin on human diseases, Food Funct 5(1) (2014) 12-17.

488 [4] W. Song, C.M. Derito, M.K. Liu, X.J. He, M. Dong, R.H. Liu, Cellular Antioxidant Activity
489 of Common Vegetables, J Agr Food Chem 58(11) (2010) 6621-6629.

490 [5] K. Pan, Y.C. Luo, Y.D. Gan, S.J. Baek, Q.X. Zhong, pH-driven encapsulation of curcumin
491 in self-assembled casein nanoparticles for enhanced dispersibility and bioactivity, Soft Matter
492 10(35) (2014) 6820-6830.

493 [6] P. Murugan, L. Pari, Influence of tetrahydrocurcumin on erythrocyte membrane bound
494 enzymes and antioxidant status in experimental type 2 diabetic rats, J Ethnopharmacol 113(3)
495 (2007) 479-486.

[7] T. Plyduang, L. Lomlim, S. Yuenyongsawad, R. Wiwattanapatapee, Carboxymethylcellulose-tetrahydrocurcumin conjugates for colon-specific delivery of a novel anti-cancer agent, 4-amino tetrahydrocurcumin, Eur J Pharm Biopharm 88(2) (2014) 351-360.

[8] A. Mahal, P. Wu, Z.H. Jiang, X.Y. Wei, Schiff Bases of Tetrahydrocurcumin as Potential Anticancer Agents, Chemistryselect 4(1) (2019) 366-369.

[9] R. Lagoa, J. Silva, J.R. Rodrigues, A. Bishayee, Advances in phytochemical delivery systems for improved anticancer activity, Biotechnol Adv 38 (2020).

[10] Z. Cong, L. Zhang, S.Q. Ma, K.S. Lam, F.F. Yang, Y.H. Liao, Size-Transformable Hyaluronan Stacked Self-Assembling Peptide Nanoparticles for Improved Transcellular Tumor Penetration and Photo-Chemo Combination Therapy, ACS Nano 14(2) (2020) 1958-1970.

[11] Q. Sun, X. Sun, X. Ma, Z. Zhou, E. Jin, B. Zhang, Y. Shen, E.A. Van Kirk, W.J. Murdoch, J.R. Lott, T.P. Lodge, M. Radosz, Y. Zhao, Integration of nanoassembly functions for an effective delivery cascade for cancer drugs, Adv Mater 26(45) (2014) 7615-21.

[12] X.Y. Wang, H.M. Huang, X.Y. Chu, Y.Q. Han, M.L. Li, G.Y. Li, X.Y. Liu, Encapsulation and binding properties of curcumin in zein particles stabilized by Tween 20, Colloid Surface A 577 (2019) 274-280.

[13] D.R.B. Oliveira, G.D. Furtado, R.L. Cunha, Solid lipid nanoparticles stabilized by sodium caseinate and lactoferrin, Food Hydrocolloid 90 (2019) 321-329.

514 [14] H.R. Kavousi, M. Fathi, S.A.H. Goli, Novel cress seed mucilage and sodium caseinate
515 microparticles for encapsulation of curcumin: An approach for controlled release, Food Bioprod
516 Process 110 (2018) 126-135.
517 [15] K. Pan, H.Q. Chen, P.M. Davidson, Q.X. Zhong, Thymol Nanoencapsulated by Sodium
518 Caseinate: Physical and Antilisterial Properties, J Agr Food Chem 62(7) (2014) 1649-1657.
519 [16] I. Belyamani, F. Prochazka, G. Assezat, Production and characterization of sodium
520 caseinate edible films made by blown-film extrusion, J Food Eng 121 (2014) 39-47.
521 [17] Z. Hosseini, K. Jalili, S. Rajabnia, L. Behboodpour, F. Abbasi, Association of amphiphilic
522 block copolymers in dilute solution: With and without shear forces, J Ind Eng Chem 72 (2019)
523 319-331.
524 [18] M. Arshad, R.A. Pradhan, A. Ullah, Synthesis of lipid-based amphiphilic block copolymer
525 and its evaluation as nano drug carrier, Mat Sci Eng C-Mater 76 (2017) 217-223.
526 [19] M. Esmaili, S.M. Ghaffari, Z. Moosavi-Movahedi, M.S. Atri, A. Sharifizadeh, M. Farhadi,
527 R. Yousefi, J.M. Chobert, T. Haertle, A.A. Moosavi-Movahedi, Beta casein-micelle as a nano
528 vehicle for solubility enhancement of curcumin; food industry application, Lwt-Food Sci
529 Technol 44(10) (2011) 2166-2172.

530 [20] F.P. Chen, B.S. Li, C.H. Tang, Nanocomplexation between Curcumin and Soy Protein
531 Isolate: Influence on Curcumin Stability/Bioaccessibility and in Vitro Protein Digestibility, J
532 Agr Food Chem 63(13) (2015) 3559-3569.
533 [21] L. Luo, Y. Wu, C. Liu, Y. Zou, L. Huang, Y. Liang, J. Ren, Y. Liu, Q. Lin, Elaboration
534 and characterization of curcumin-loaded soy soluble polysaccharide (SSPS)-based nanocarriers
535 mediated by antimicrobial peptide nisin, Food Chem 336 (2021) 127669.
536 [22] Y.B. Yu, W.D. Cai, Z.W. Wang, J.K. Yan, Emulsifying properties of a ferulic acid-grafted
537 curdlan conjugate and its contribution to the chemical stability of beta-carotene, Food Chem
538 339 (2021) 128053.
539 [23] A.F. Martins, P.V. Bueno, E.A. Almeida, F.H. Rodrigues, A.F. Rubira, E.C. Muniz,
540 Characterization of N-trimethyl chitosan/alginate complexes and curcumin release, Int J Biol
541 Macromol 57 (2013) 174-84.
542 [24] F. Liao, L. Liu, E. Luo, J. Hu, Curcumin enhances anti-tumor immune response in tongue
543 squamous cell carcinoma, Arch Oral Biol 92 (2018) 32-37.
544 [25] K.L. Wolfe, R.H. Liu, Cellular antioxidant activity (CAA) assay for assessing antioxidants,
545 foods, and dietary supplements, J Agr Food Chem 55(22) (2007) 8896-8907.

546 [26] Y. Wei, F. Vriesekoop, Q. Yuan, H. Liang, beta-Lactoglobulin as a Nanotransporter for
547 Glabridin: Exploring the Binding Properties and Bioactivity Influences, ACS Omega 3(9)
548 (2018) 12246-12252.
549 [27] Z. Liu, Q. Wu, J. He, F. Vriesekoop, H. Liang, Crystal-Seeded Growth of pH-Responsive
550 Metal–Organic Frameworks for Enhancing Encapsulation, Stability, and Bioactivity of
551 Hydrophobicity Compounds, ACS Biomaterials Science & Engineering 5(12) (2019)
552 6581-6589.
553 [28] O.A.K. Khalil, O.M.M.D. Oliveira, J.C.R. Vellosa, A.U. de Quadros, L.M. Dalposso, T.K.
554 Karam, R.M. Mainardes, N.M. Khalil, Curcumin antifungal and antioxidant activities are
555 increased in the presence of ascorbic acid, Food Chem 133(3) (2012) 1001-1005.
556 [29] K. Pan, Q.X. Zhong, S.J. Baek, Enhanced Dispersibility and Bioactivity of Curcumin by
557 Encapsulation in Casein Nanocapsules, J Agr Food Chem 61(25) (2013) 6036-6043.
558 [30] L. Maldonado, R. Sadeghi, J. Kokini, Nanoparticulation of bovine serum albumin and
559 poly-d-lysine through complex coacervation and encapsulation of curcumin, Colloids Surf B
560 Biointerfaces 159 (2017) 759-769.
561 [31] Y. Zhang, F. Yao, J. Liu, W. Zhou, L.L. Yu, Synthesis and characterization of alkylated
562 caseinate, and its structure-curcumin loading property relationship in water, Food Chem 244
563 (2018) 246-253.

564 [32] T. Feng, K. Wang, F.F. Liu, R. Ye, X. Zhu, H.N. Zhuang, Z.M. Xue, Structural
565 characterization and bioavailability of ternary nanoparticles consisting of amylose,
566 alpha-linoleic acid and beta-lactoglobulin complexed with naringin, Int. J. Biol. Macromol. 99
567 (2017) 365-374.
568 [33] S. Dey, A. Schonleber, S. Mondal, S.I. Ali, S. van Smaalen, Role of Steric Hindrance in
569 the Crystal Packing of Z '=4 Superstructure of Trimethyltin Hydroxide, Cryst. Growth Des.
570 18(3) (2018) 1394-1400.
571 [34] H. Souguir, F. Salaun, P. Douillet, I. Vroman, S. Chatterjee, Nanoencapsulation of
572 curcumin in polyurethane and polyurea shells by an emulsion diffusion method, Chem Eng J
573 221 (2013) 133-145.
574 [35] T.F. Kumosinski, J.J. Unruh, Quantitation of the global secondary structure of globular
575 proteins by FTIR spectroscopy: Comparison with X-ray crystallographic structure, Talanta
576 43(2) (1996) 199-219.
577 [36] H.R. Park, S.J. Rho, Y.R. Kim, Solubility, stability, and bioaccessibility improvement of
578 curcumin encapsulated using 4-alpha-glucanotransferase-modified rice starch with reversible
579 pH-induced aggregation property, Food Hydrocolloid 95 (2019) 19-32.
580 [37] A.A. Adwa, A.S.I. Elsayed, A.E. Azab, F.A. Quwaydir, Oxidative stress and antioxidant
581 mechanisms in human body., J Appl Biotechnol Bioeng 6 (2019) 43-47.

582 [38] H. Zhang, W. Jiang, R. Liu, J. Zhang, D. Zhang, Z. Li, Y. Luan, Rational Design of Metal
583 Organic Framework Nanocarrier-Based Codelivery System of Doxorubicin
584 Hydrochloride/Verapamil Hydrochloride for Overcoming Multidrug Resistance with Efficient
585 Targeted Cancer Therapy, ACS Appl Mater Interfaces 9(23) (2017) 19687-19697.
586 [39] L. Xiang, Y. Nakamura, Y.M. Lim, Y. Yamasaki, Y. Kurokawa-Nose, W. Maruyama, T.
587 Osawa, A. Matsuura, N. Motoyama, L. Tsuda, Tetrahydrocurcumin extends life span and
588 inhibits the oxidative stress response by regulating the FOXO forkhead transcription factor,
589 Aging-Us 3 (2011) 1098-1109.
590 [40] C. Syng-ai, A.L. Kumari, A. Khar, Effect of curcumin on normal and tumor cells: Role of
591 glutathione and bcl-2, Mol Cancer Ther 3(9) (2004) 1101-1108.
592 [41] T. Choudhuri, S. Pal, T. Das, G. Sa, Curcumin selectively induces apoptosis in deregulated
593 cyclin D1-expressed cells at G(2) phase of cell cycle in a p53-dependent manner, J Biol Chem
594 280(20) (2005) 20059-20068.
595 [42] P.Y. Chang, S.F. Peng, C.Y. Lee, C.C. Lu, S.C. Tsai, T.M. Shieh, T.S. Wu, M.G. Tu, M.Y.
596 Chen, J.S. Yang, Curcumin-loaded nanoparticles induce apoptotic cell death through regulation
597 of the function of MDR1 and reactive oxygen species in cisplatin-resistant CAR human oral
598 cancer cells, Int J Oncol 43(4) (2013) 1141-1150.

599 [43] L. Bechnak, C. Khalil, R. El Kurdi, R.S. Khnayzer, D. Patra, Curcumin encapsulated
600 colloidal amphiphilic block co-polymeric nanocapsules: colloidal nanocapsules enhance
601 photodynamic and anticancer activities of curcumin, Photochemical & Photobiological
602 Sciences 19(8) (2020) 1088-1098.
603 [44] G. Zhao, X. Han, S. Zheng, Z. Li, Y. Sha, J. Ni, Z. Sun, S. Qiao, Z. Song, Curcumin
604 induces autophagy, inhibits proliferation and invasion by downregulating AKT/mTOR
605 signaling pathway in human melanoma cells, Oncol Rep 35(2) (2016) 1065-74.
606 [45] W. Liu, Z. Zhang, G. Lin, D. Luo, H. Chen, H. Yang, J. Liang, Y. Liu, J. Xie, Z. Su, H.
607 Cao, Tetrahydrocurcumin is more effective than curcumin in inducing the apoptosis of H22
608 cells via regulation of a mitochondrial apoptosis pathway in ascites tumor-bearing mice, Food
609 Funct 8(9) (2017) 3120-3129.
610 [46] S. Awasthi, U. Pandya, S.S. Singhal, J.T. Lin, V. Thiviyanathan, W.E. Seifert Jr, Y.C.
611 Awasthi, G.A.S. Ansari, Curcumin glutathione interactions and the role of human glutathione
612 S-transferas., Chemico-Biological Interaction 128 (2000) 19-38.
613 [47] P. Yoysungnoen, P. Wirachwong, C. Changtam, A. Suksamram, S. Patumraj, Anti-cancer
614 and anti-angiogenic effects of curcumin and tetrahydrocurcumin on implanted hepatocellular
615 carcinoma in nude mice, World J Gastroentero 14(13) (2008) 2003-2009.
616

BEIJING UNIVERSITY OF CHEMICAL TECHNOLOGY

Response to Reviewers

Dear Editor and Reviewers:

Thank you for your letter and for the reviewers' comments concerning our manuscript, entitled “Designing biocompatible protein nanoparticles for improving the cellular uptake and antioxidation activity of Tetrahydrocurcumin.” (Manuscript Number: JDDST-D-20-00777). These comments are all valuable and very helpful for revising and improving our paper, as well as the important guiding significance to our researches. We tried our best to revise the manuscript according to the reviewers’ comments. Revised portion are highlighted in RED in the revised manuscript. The main corrections in the paper and the responds to the reviewer's comments are as following:

To Reviewer #1:

We thank you so carefully review of our manuscript and recommending publish of this manuscript. Each of your comments is vital to the improvement of the quality of the article. We tried our best to revise the manuscript according to your comments. Revised portion are highlighted in RED in the revised manuscript.

Comment 1

The purpose of this study is to develop one method for the preparation of biocompatible protein nanoparticles with advantages, such as increased water solubility of THC, enhanced cellular absorption and antioxidant activity, etc. However, I suggest that the transport or metabolic pathways of the protein nanoparticles is necessary to reveal the complementary mechanisms of action.

ANSWER:

Thank you for your valuable advice. The study of the transport and metabolic pathway of protein nanoparticle is indeed necessary to reveal the mechanism of action. From previous studies, we also know that nanoparticle enter cell mainly through five steps and then are degraded by intracellular lysosomes to release drugs. In the introduction part, we explain the transport process of nano-delivery system.

Beijing University of Chemical Technology, No. 15, Bei San Huan Dong Rd., Beijing 100029, China
Tel: +86-10-6443-1557 Fax: +86-10-6443-7610

Comment 2

The preparation method of the sample solution is described in the manuscript, but there is no description on how solid samples were obtained for characterization. Effect of solvent and extraction process on crystal morphology should be considered and compared with free THC.

ANSWER:

Thank you for your valuable advice. Our solid samples are obtained by freeze-drying. We also made a supplementary explanation in the manuscript and the freeze-drying process does not use solvent.

Comment 3

The characterization method and results adopted in the study cannot strongly prove the packaging method of the sample, so I suggest perfecting these work.

ANSWER:

We thank you so carefully review of our manuscript. The formation of THC@NaCas is mainly through interaction between molecules. It is a self-assembly process. The characterization methods (FTIR, XRD and DLS) adopted in the study can be well prove that THC was successfully packaged into NaCas. The crystal form and functional groups of substances have changed after encapsulation. The particle size also increases correspondingly.

Comment 4

The stability of the new drug loading method and the influence of the pH value of the solution should be considered in the solubility experiment.

ANSWER:

Thank you for pointing this out. Your advice was very meaningful. I have included the stability study of THC@NaCas in the appropriate places in the manuscript. (please see 2.4 and 3.2)

Comment 5

It is necessary to determine the optimal ratio of THC to NaCas through experiments and introduce the method of removing excessive free NaCas.

ANSWER:

Thank you for pointing this out. We explored the optimal ratio of THC and NaCas , but we did not give it in detail in the original manuscript. According to your suggestion, we summarized the LC% and EE% in different ratio of THC to NaCas in table 1. We finally chose the conditions with the highest entrapment efficiency and loading efficiency. In the experiment, we tried our best to choose NaCas at a low concentration.

Comment 6

Recommend describing the possible clinical applications of this protein nanoparticle and the prospects for improving the biological activity of hydrophobic drugs in this manner.

ANSWER:

Thank you for your valuable advice. In conclusion section, I explained in detail the possible clinical applications and prospects of nanoparticles.

To Reviewer #2:

We thank you so carefully review of our manuscript and recommending publish of this manuscript. Each of your comments is vital to the improvement of the quality of the article. We tried our best to revise the manuscript according to your comments. Revised portion are highlighted in RED in the revised manuscript.

Comment 1

The authors have reported the preparation of NaCas nanoparticles, but the detailed methodology for optimizing the process is not given. I would suggest the authors to mention why they chose only 200 mg of NaCas in 100 ml water, why not 100 mg. Also on what basis did they decided to stir the solution for 4 hrs.

ANSWER:

We acknowledge your comments and suggestions very much, which are valuable in improving the quality of our manuscript. The optimizing the process is given in revised manuscript. Table 1 summarizes the encapsulation efficiency and loading capacity of THC under all conditions. When the concentration of NaCas and THC is 2mg/mL, the obtained nanoparticles have the highest entrapment efficiency and loading efficiency.

According to previous studies, the formed nanoparticles after stirring for 4 hours are more stable. Therefore, we set the mixture solution of THC and NaCas was stirred for 4 hrs.

Comment 2

The cellular uptakes of nanoparticles are size dependent. What is the size of the nanoparticle. The authors need to characterize the size and stability of the nanoparticles.

ANSWER:

Thank you for pointing this out. The size and stability of the nanoparticles were characterized in the revised manuscript. (please see the supplementary file)

Comment 3

Generally, NaCas nanoparticles are stabilized in presence of calcium ions. How stable is the nanoparticles in absence of Ca2+ ions.

ANSWER:

We thank you so carefully review of our manuscript. The particle size of THC@NaCas in absence of Ca2+ ions is 269 nm, ζ-potential is -21.3 mV (please see supplementary files). High surface potenbtial and small particle size make THC@NaCas stable.

Comment 4

What is the surface charge on the nanoparticles in presence and absence of THC. It is important to check the zeta potential of the nanocarrier.

ANSWER:

Thank you for pointing this out. The ζ-potential of the NaCas and THC@NaCas were characterized in the revised manuscript. (please see supplementary file)

Beijing University of Chemical Technology, No. 15, Bei San Huan Dong Rd., Beijing 100029, China
Tel: +86-10-6443-1557 Fax: +86-10-6443-7610

Comment 5

The encapsulation of the drug is done by UV-Visible at 280 nm. There may be some contamination of the protein during estimating the drug at 280 nm. It is known that tyrosine has absorbance at 280 nm. The best method to estimate the amount loaded in the nanocarrier is by using HPLC. Also the absorption spectras of blank NaCas, THC and THC encapsulated in NaCas must be recorded and given in the manuscript.

ANSWER:

We thank you so carefully review of our manuscript. The encapsulation efficiency of THC was tested by re-dissolving precipitation with ethanol and then measuring the absorbance using UV-Visible at 280 nm. It is feasible because the precipitation is only free THC and no NaCas. Also the absorption spectras of blank NaCas, THC and precipitation were given in the supplementary files. In the subsequent determination of loading capacity of THC, we adopt HPLC to test in order to avoiding interference of NaCas.

Comment 6

Entrapment efficiency depends on the amount of the initial drug taken and so it can vary with change in the drug concentration. For better comparison, along with entrapment efficiency, the authors should also mention the loading capacity of the nanocarrier.

ANSWER:

Thank you for pointing this out. The loading capacity of THC@NaCas was added to the revised manuscript. (please see Table 1)

Comment 7

The authors have used KBr pallet to measure the FTIR spectra of the drug loaded nanocarrier. What was the procedure, whether drop of NaCas@THC solution was dropped on KBr or the solution was lyophilized. If lyophilized what was the cryoprotectant used in lyophilisation process

ANSWER:

We thank you so carefully review of our manuscript. The operation procedure of FTIR: First, freeze-drying THC@NaCas solution to get THC@NaCas solid powder, and

then mix THC@NaCas solid powder with KBr solid powder. Finally, the mixture will be pressed into thin slices using professional equipment.

Comment 8

The authors have used the term "loading efficiency of the drug in NaCas was evaluated by FTIR and XRD". The term loading efficiency is used to quantify the amount of drug loaded. How can these two techniques tell the quantity of the drug loaded in the nanocarrier. They should modify the statement.

ANSWER:

Thank you for pointing this out. XRD and FTIR were used to identify whether THC was successfully encapsulated into NaCas to form a composite nanoparticle structure. The word "efficiency" may not be appropriate in manuscript, we have made correct modification.

Comment 9

Additionally to show the enhance utility of the nanocarrier, I would suggest the authors to perform the in vitro drug release kinetics of the nanocarrier in normal saline and stimulated gastric fluid condition

ANSWER:

We acknowledge your comments and suggestions very much, which are valuable in improving the quality of our manuscript. We studied the in vitro release kinetics of THC@NaCas in normal saline and stimulated gastric fluid in revised manuscript. (please see 2.5 and 3.3)

Comment 10

On page 22, line 288: The statement " but the growth-stimulation effect did not persist at any of the higher THC@NaCas concentrations": please mention at what concentration and why does it does not show stimulated growth unlike the free THC.

ANSWER:

Thank you for your question, this question is very meaningful for our research. When the concentration of THC@NaCas is above 2 μg/mL, the growth-stimulation effect is not significant. Our experimental results did show different stimulating effects of free THC and THC@NaCas. We will continue to explore this in depth in the future.

Comment 11

Page 23, line 303: Curcumin posses α, β-unstauated double bond conjugated with keto group. This feature is responsible for its reaction with glutathione by known Micheal addition reaction. In case of THC, there is no double bond and hence these don't react with GSH and thus are metabolically more stable. The reference no 37 given in the manuscript mentions about the reaction of curcumin with GSH and not THC. In fact there are reports which states that THC elevates GSH (Murugan P, Pari L. Antioxidant effect of tetrahydrocurcumin in streptozotocin-nicotinamide induced diabetic rats. Life Sci. 2006 Sep 27;79(18):1720-8.) or has no adverse effect on the concentration of GSH (Atsumi T, Tonosaki K, Fujisawa S. Comparative cytotoxicity and ROS generation by curcumin and tetrahydrocurcumin following visible-light irradiation or treatment with horseradish peroxidase. Anticancer Res. 2007 Jan-Feb;27(1A):363-71). The authors need to modify the statement.

ANSWER:

Thank you for your question, this question is very meaningful for our research. After reviewing a large number of literatures, we refined the mechanism of THC against A375 cell. (Please see red part in 3.5)

Comment 12

Along with the above scientific content, the authors need to check grammatical content and typographical error. For example the spelling of reference is incorrect in the manuscript.

Page 4, line 60: Delete the word "are"

Page 3: Line 42 : Free radicals are not just atoms, please change the word "atomic orbit"

The general abbreviation prevalent for 2,2-Azobis(2-amidinopropane)-dihydrochloride is AAPH. The authors can change the abbreviation from ABAP to AAPH.

ANSWER

Page 4, line 60: Delete the word “are” in revise manuscript.

Page 3, line 42: Delete the word “atomic” in revise manuscript.

All “ABAP” in the article has been replaced with “AAPH”

We acknowledge your comments and suggestions very much, which are valuable in improving the quality of our manuscript.

We have carefully revised the manuscript according to the reviewers’ comments and also have re-scrutinized to improve the English by the native speakers. We checked the grammar and corrected it. Revised portion are highlighted in RED in the revised manuscript. We appreciate for Editors/Reviewers’ warm work earnestly, and hope that the correction will meet with approval.

Yours Sincerely

Hao Liang

Beijing University of Chemical Technology

RESEARCH HILIGHTS

- Tetrahydrocurcumin loaded protein nanoparticles were successfully prepared by precipitation.
- The protein-based carrier awarded an encapsulation efficiency and greater solubility.
- The nanoparticles facilitated a high cellular uptake and enhanced the antioxidant activity.

Graphical Abstract

Designing Biocompatible Protein Nanoparticles for Improving the Cellular Uptake and Antioxidation Activity of Tetrahydrocurcumin.

Shan Chen[a], Qiao Wu[a], Mengyan Ma, Zezhong Huang, Hao Liang[*, a], Frank Vriesekoop.

[a] State Key Laboratory of Chemical Resource Engineering, Beijing University of Chemical Technology, Beijing, P. R. China

Corresponding Author: [*]Prof Hao Liang, State Key Laboratory of Chemical Resource Engineering, Beijing University of Chemical Technology, Beisanhuan Donglu 15 Hao, Beijing, P. R. China

Tel.: +861064431557; Fax: +861064437610. Email address: lianghao@mail.buct.edu.cn

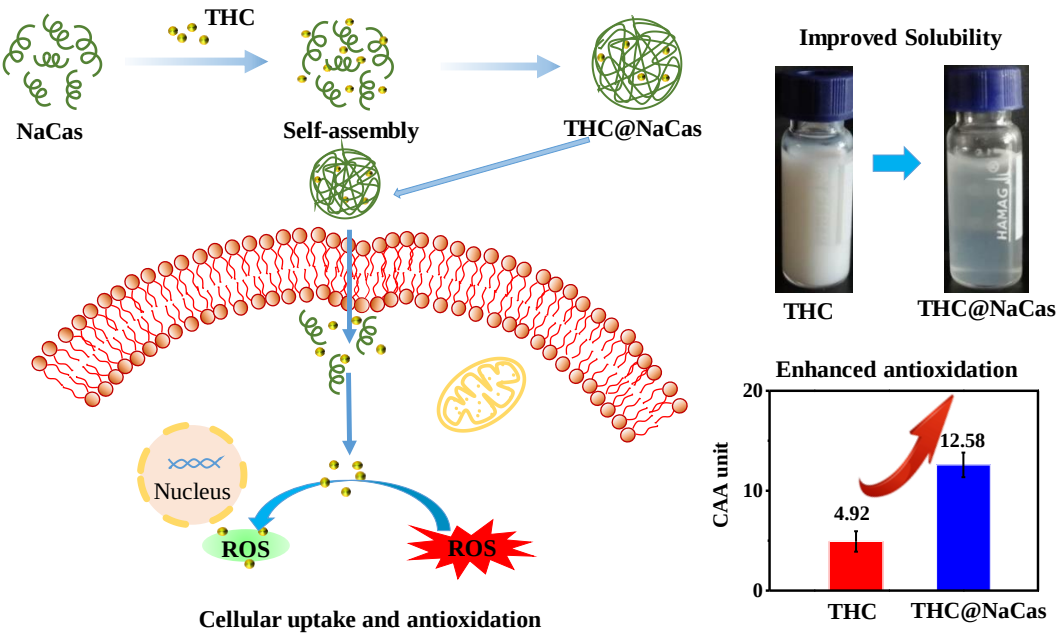
THC
NaCas
Self-assembly
THC@NaCas
Nucleus
ROS
ROS
Cellular uptake and antioxidation
Improved Solubility
THC
THC@NaCas
Enhanced antioxidation
CAA unit
20
10
0
4.92
12.58
THC
THC@NaCas

Declaration of interests

☐ √ The authors declare that they have no known competing financial interests or personal relationships that could have appeared to influence the work reported in this paper.

☐The authors declare the following financial interests/personal relationships which may be considered as potential competing interests:

Shan Chen: Conceptualization, Methodology, Software, Writing, Data collection**. Qiao Wu**: Experimental guidance, Supervision. **Mengyan Ma**: Sample preparation. **Zezhong Huang**: Sample preparation. **Frank Vriesekoop:** Language revision. **Hao Liang**: Language revision.

Click here to access/download
Supplementary Material
Supplementary files.docx

Revised Manuscript (Clean Version) Click here to view linked References

Designing biocompatible protein nanoparticles for improving the cellular uptake and antioxidation activity of Tetrahydrocurcumin.

Shan Chen [a], Qiao Wu [a], Mengyan, Ma [a], Zezhong, Huang [a], Frank Vriesekoop [c, *], and Hao Liang [a, b,*]

[a] *State Key Laboratory of Chemical Resource Engineering, Beijing University of Chemical Technology, Beijing 100029, P. R. China*

[b] *Qinhuangdao Bohai Biological Research Institute of Beijing University of Chemical Technology,Qinhuangdao 066000, China*

[c] *Department of Food Technology and Innovation, Harper Adams University, Newport TF10 8NB, Shropshire, England*

Corresponding Author

* E-mail: lianghao@mail.buct.edu.cn (Hao Liang);

FVriesekoop@harper-adams.ac.uk (Frank Vriesekoop)

Abstract:

Tetrahydrocurcumin (THC) is a natural molecule with anticancerous, antioxidant and other beneficial activities. However, its low aqueous solubility leads to poor bioavailability. Sodium caseinate (NaCas) is an ideal natural protein carrier with amphiphilic and non-toxic properties, which provides a new possibility for improving the aqueous solubility of THC. In this study, THC loaded protein nanoparticles (THC@NaCas) were successfully prepared by a nanoprecipitation method. The protein-based carrier awarded an encapsulation efficiency of about 98 % for THC. The structure and physicochemical characteristics of THC@NaCas nanoparticles were characterized by Fourier Transform Infrared Spectroscopy (FTIR), X-ray diffraction, and Scanning Electron Microscopy (SEM). The solubility test comfirmed that protein nanoparticles awarded greater solubility of THC. Furthermore, THC@NaCas had a greater antioxidant activity compared to free THC, resulting in a free radical scavenging ability of THC@NaCas 2.6 times greater than that of free THC. The *in vitro* cytotoxicity test showed that the THC@NaCas nanoparticles had a stronger inhibitory effect on cancer cells compared with free THC, and good biocompatibility for non-cancerous cells. In a short, Our results demonstrate that protein-based nanoparticles have the potential to improve the bioactivity of hydrophobic drugs in clinical application.

35 Keywords: Sodium Caseinate; Tetrahydrocurcumin; Nanoparticles; Cellular uptake;
36 Antioxidant

37

38 **1. Introduction**

39 Oxidative stress, induced by free radicals produced through normal cellular metabolism, has
40 been suggested to be a factor contributing to the development of various diseases such as
41 diabetes, cancer, atherosclerosis and neurodegeneration, and the accelerated onset of aging [1-3].
42 Free radicals, which have a single unpaired electron in their outer orbit, are able to damage and
43 alter a range of biomolecules including lipids, nucleic acids, and proteins in the body,
44 potentially leading to the onset of the above mentioned disorders [3, 4]. Therefore, there is an
45 urgent need for a drug or natural ingredient to eliminate the excessive free radicals produced in
46 the body.

47 Various phytochemicals possess properties that have antioxidant, anti-inflammatory, and
48 anti-cancerous properties [5]. Tetrahydrocurcumin (THC), a major metabolite of curcumin, has
49 displayed the ability to prevent oxidative effects caused by various diseases and has been shown
50 to possess anti-cancerous properties [3]. THC exhibits a greater antioxidant activity *in vivo*
51 systems when compared with curcumin and has shown the potential to control free radicals by
52 protecting cells against oxidative stress by trapping free radicals produced during diabetes [6].

In a clinical study conducted on male diabetic Wistar rats, THC was found to have a positive impact on erythrocyte membrane bound enzymes by imposing an antioxidant defence [6]. Compared with curcumin, THC is significantly more potent under physiological conditions, has higher antioxidant activity, and induces a more effective tumor angiogenesis [7, 8]. However, THC has poor aqueous solubility, degrades rapidly on exposure to oxygen and is poorly absorbed in the gastrointestinal tract, which hinders its dietary/nutraceutical application [5, 9]. Hence the requirement for the development of a natural delivery system can overcome the disadvantages in the efficient delivery of THC.

It has been reported that the delivery of active drugs to the cytoplasm of tumor cells must go through five steps. (1) Nanoparticles are transported through the blood circulation. (2) The permeability of nanoparticles makes them accumulate in tumor site. (3) Gradually penetrate into tumor tissue. (4) Nanoparticles are internalized by tumor cells via endocytosis. (5) Active drug release via lysosome [10, 11]. Therefore, ideal drug delivery systems have a high drug loading efficiency and nanocarriers with large surface area to volume ratio which improve the delivery of the drug to the required tissues/cells [9]. The biocompatibility and efficiency of natural compounds, which are now considered key components in the prevention of diseases such as cancer, diabetes, and inflammation, are markedly improved through the creation of protein-based delivery systems [3]. In a protein-based drug delivery system, proteins are used

as stable encapsulation carriers with the ability to improve dispersion, protect the compounds they carry and improve the physical stability of these compounds in a range of environments [9, 12]. Sodium caseinate's amphiphilic tendencies makes it an effective protein used in drug delivery systems [13]. Sodium caseinate (NaCas), is derived from caseinate, a protein typically derived from bovine milk [14, 15]. NaCas is produced following the precipitation of casein at its isoelectric point (pH 4.6) and the readjustment of the pH to 6.7 using sodium hydroxide [16]. Due to its high content of hydrophobic amino acids, NaCas has emulsifying properties which makes it as a naturally occurring amphiphilic block copolymer [5, 13]. Amphiphilic block copolymers exhibit both immiscibility in water and hydration tendencies, properties that are necessary to encapsulate hydrophobic bioactive compounds such as THC [5, 17]. Amphiphilic block copolymers are commonly used for drug delivery systems, specifically as carriers for nanomedicine [18], which self-assemble in aqueous solutions to form micelles [17]. When the NaCas micelles self-assemble they can encase the hydrophobic bioactive compounds, the micelles then act as an effective carrier to improves the dispersibility of the encapsulated guest compounds in aqueous solution [17-20].

In this study, sodium caseinate was employed to encapsulate THC in a green and safe self-assembled manner to facilitate an enhanced cellular uptake and antioxidant activity (**Scheme 1**). The efficiency of THC incorporation into NaCas was assessed by means of Fourier

Transform Infrared (FTIR) spectroscopy and X-Ray Diffraction (XRD), following which the encapsulated THC was evaluated for its antioxidant capabilities and cell uptake through testing on non-cancerous embryonic cells (3T3 cells) and cancerous melanoma cell (A375 cells). Our results showed that the cell uptake and antioxidant capabilities of THC were significantly improved and the prepared nanoparticles had good biocompatibility.

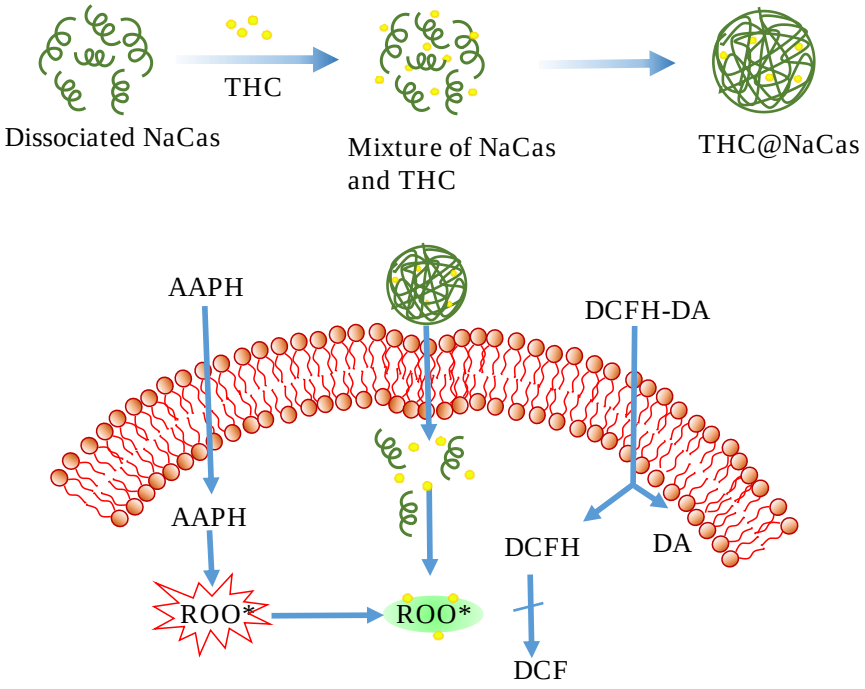

Scheme 1: Schematic representation of the synthesis, cellular uptake and cellular antioxidant activity of THC@NaCas. After the DCFH-DA entered the cells, it cleaved into DA and DCFH, AAPH decomposed and produced free radicals, which could transform DCFH into fluorescent DCF, THC@NaCas were able to scavenge the free radicals to reducing the production of DCF.

2. Materials and methods

2.1. Materials

2,2-Azobis(2-amidinopropane)-dihydrochloride (AAPH) and 2,7-dichlorodi-hydro-fluorescein diacetate (DCFH-DA) were obtained from Sigma-Aldrich (St. Louis, MO, USA). Sodium caseinate (NaCas) and tetrahydrocurcumin (THC) were purchased from Mackin Biochemical (Shanghai, China). L-tyrosine (25KU, from mushroom) was supplied by Aladdin Inc. (Shanghai, China). Dimethyl sulfoxide (DMSO) was bought from Sinopharm Chemical Reagent Co., Ltd (Shanghai, China). Cell Counting Kit-8 (CCK-8) was purchased from Dojindo Laboratories (Tokyo, Japan). 3T3 cells (Mouse embryonic fibroblasts) and A375 cells (Human melanoma cells) were got from the Cell Resource Center, Peking Union Medical College (Beinjing, China). The cell culture medium was DMEM with 10 % Fetal Bovine Serum, and the cells were incubation with 5 % CO_2 and 95 % air at 37 ºC. All other materials were obtained from Beijing Biochemical (Beijing, China).

2.2. Synthesis of THC@NaCas

The THC stock solution was prepared by dissolving 20 mg of THC in 10 mL ethyl alcohol. The NaCas stock solution was prepared by dissolving 200 mg of NaCas in 100 mL deionized water under vigorous stirring for 30 minutes. To create the THC@NaCas, 10 mL of THC

118 solution was dropwise added into 100 mL of NaCas solution under vigorous stirring for 4 hours
119 at room temperature. Then the mixed solution was centrifuged at 400 g for 10 minutes. The
120 supernatant contained THC@NaCas and the precipitation was THC which had not been
121 successfully encapsulation. Followed, the un-encapsulated THC was measured using
122 UV-visible spectrophotometer (Shimadzu, UV-2450, Japan) at 280nm in order to evaluate the
123 encapsulation efficiency (EE). Then the supernatant was freeze-dried to obtain solid powder
124 and used to determine THC loading capacity (LC). The LC of THC was tested by high
125 performance liquid chromatography (HPLC) (LC-15C, Japan) with a detection wavelength is
126 280 nm. Acetonitrile and phosphoric acid aqueous solution (50:50, v/v) were used as a mobile
127 phase. Ethanol was used to extract the encapsulated THC from the protein nanoparticles, and
128 then the ethanol solution was filtered by 0.22 μm membrane to remove the insoluble protein.
129 The EE and LC were calculated according to the following equations:

130 $$\text{EE}\ (\%) = \frac{total\ amount\ of\ added\ THC - amount\ of\ THC\ on\ the\ bottom}{total\ amount\ of\ added\ THC} \times 100\%$$

131

132 $$\text{LC}\ (\%) = \frac{\text{amount of THC loaded}}{total\ amount\ of\ NPs} \times 100\%$$

133

134 ***2.3. Characterization of THC@NaCas***

135 The particle size and zeta potential of NaCas and THC@NaCas were measured using a

dynamic light scattering instrument at 25 ºC (Mastersizer 2000, Malvern Instruments Ltd., Malvern, Worcestershire, UK). Before the measurement, a certain amount of solid powder was diluted with deionized water. Each set of data was collected by balancing the emulsion in the measuring room for 120 s.

The morphology of NaCas and THC@NaCas was recorded using a HITACHI S-4700 scanning electron microscope (SEM) (Tokyo, Japan). All samples were attached to brass stubs with double-sided tape before sputtered-coated with a thin gold layer for analysis.

The X-ray diffraction patterns of THC, NaCas and THC@NaCas were recorded on an X-ray diffractometer (Bruker, D8 ADVANCE, Karlsruhe, Germany) equipped with a copper target X-ray tube. The voltage and current applied were set at 40 kV and 40 mA, respectively. The diffraction angles were scanned from 5° to 90° in 2θ at a scan rate of 10°/min and a step of 0.02°.

A FTIR spectrometer (JASCO FT-IR 6600, Madison, WI, USA) equipped with a DLaTGS detector was used to investigate the changes in the secondary structure of the NaCas as well as the dynamics of its interaction with THC. THC, NaCas and THC@NaCas were pressed into KBr salt tablets at 10 mg sample per g of KBr with the spectrometric scanning range between 4000 and 400 cm^{-1}.

In order to determine the effect of temperature and concentration on the solubility of

154 THC@NaCas in water, various amounts of THC@NaCas powder were dissolved in 20 mL
155 deionized water. The final concentrations of THC@NaCas suspensions were 0, 10, 20, 30, 40,
156 50 mg/mL. The THC@NaCas suspensions were agitated in an orbital shaking incubator at 100
157 rpm for 30 min at either 25 °C or 37 °C, following which samples were filtered through a 0.22
158 μm membrane to remove any insoluble substances. 500 μL of the filtrate was taken and diluted
159 with absolute ethanol to 12.5 mL. The absorbance was measured at 280 nm UV-visible
160 spectrophotometer (Shimadzu, UV-2450, Japan) and the THC dissolution was calculated
161 compared with the standard curve ranging from 6 to 14 μg/mL THC which had a correlation
162 coefficient of R^2>0.994 (Figure S1).
163
164 ***2.4. Stability evaluation of THC@NaCas***
165 Thermal stability and pH stability of free THC and THC@NaCas were determined according
166 to previous research methods [21, 22] with appropriate modification. Two solutions containing
167 the same amount of THC were placed at 80 ºC water bath and heated continuously for several
168 hours. Taking out a certain volume of liquid every half an hour and detecting THC content by
169 high performance liquid chromatography (HPLC). Similarly, a certain amount of THC@NaCas
170 solid powder and free THC were dissolved into different phosphate buffer solution respectively
171 (pH=7.0 and pH=5.4) for 2 hours. Finally, the retention rate was selected as the index to reflect

the stability of THC, the initial concentration of THC in all samples was set as 100 %.

2.5. In vitro release of THC@NaCas

The *in vitro* release kinetics of THC@NaCas in stimulated gastric fluid and normal saline were studied according to previous method [23] with appropriate modification. First, 50 mg THC@NaCas freeze-dried powder was dissolved in deionized water and dispersed in dialysis bag (MWCO, 3500Da). The dialysis bag was soaked in 200 mL stimulated gastric fluid (SGF, 2.0 mg/mL NaCl, 3.8 mg/mL pepsin and hydrochloric acid adjusts pH to 1.2) or saline solution (pH=7.0) and was stirred slowly at the speed of 100 rpm under 37 ºC. A certain time interval, 1 mL solution was extracted and added the same volume of fresh solution.

2.6. Cellular uptake of THC@NaCas

The intracellular delivery of THC@NaCas was evaluated by Confocal Laser Scanning Microscope. Cultured human melanoma cells (A375 cells) were allowed to attach to the surface of the laser confocal dish for 12 h. Then the cells were treated with equal concentration of free THC or THC@NaCas (2 mL, 5 μg/mL) for 6 h, after which the cells were washed using fresh PBS and then fixed by adding a 4% paraformaldehyde solution. Finally, the cells were stained by adding 200 μL the nucleus-staining 4,6-diamidino-2-phenylindole (DAPI) dye for 15 min.

The confocal laser scanning microscope images were obtained by exciting THC and DAPI at 405 nm, with emissions measured at 410 nm and 460 nm respectively.

2.7. Cell toxicity test

The relative toxicity of free THC and THC@NaCas were tested on non-cancerous mouse embryonic cells (3T3 cells) and cancerous human melanoma cells (A375 cells) according to a modified CCK-8 method described elsewhere [24]. Both cell types were inoculated at a density of 6×10^4 cell/well in 96-well microplates and incubated at 37 °C for 24 h, containing 50 μL of cell suspension and 50 μL different concentrations of THC (at 0, 1, 2, 3, 4, 5 μg/mL) and THC@NaCas (also at 0, 1, 2, 3, 4, 5 μg THC-equivalent/mL). Progression in cell growth was determined by measuring the optical density 450 nm by UV-VIS spectrophotometer. Three independent experiments were run with nearly identical results. The cell survival rate was calculated according to the following equations:

$$\text{Cell survival rate}(\%) = \frac{\text{Abs } treatment}{\text{Abs } blank} \times 100\%$$

2.8. Cell antioxidant capacity test

The cellular antioxidant activity (CAA) of THC@NaCas was determined by the CAA method according to Wolf and Liu [25] and modified appropriately. Both cell types (3T3 cells

and A375 cells) were seeded at a density of 6×10^4 cell/well on 96-well microplates (100 μL per well). Each sample was treated with 10 μL of THC or THC@NaCas solution at various concentrations, plus 5 μL of 2′,7′-dichlorodihydrofluorescein diacetate (DCFH-DA) (25 μM). After incubation at 37 ºC for one hour, each sample was treated with 2,2′-azobis (2-amidinopropane) dihydrochloride (AAPH) (1.2 mM, 100 μL). Samples were then incubated for one hour at 37 °C with the fluorescence being measured every 5 min at the excitation wavelength of 538 nm and the emission wavelength of 485 nm [25]. Following this, the quantification of CAA was undertaken according to Wolfe and Lui [25] using the following equation:

$$\mathrm{CAA(unit)} = 100 - \frac{\int \mathrm{SA}}{\int \mathrm{CA}} \times 100$$

Where ∫ SA represents the integrated area under sample time-fluorescence curve; while ∫ CA represents the integrated area from control curve.

2.9. Tyrosinase inhibition experiment

THC is a known inhibitor of tyronase [26], as such we investigated the inhibitory influence of both free and encapsulated THC on tyrosinase activity. The THC@NaCas nanoparticles were prepared by mixing 1mL of NaCas (2.0 mg/mL) with 100 μL of THC (2.0 mg/mL), which was vigorously stirred by means of a magnetic stirrer for 30 min. From this stock solution four

THC@NaCas nanoparticles samples were diluted with PBS to different concentrations of THC (5, 10, 15 and 20 μg /mL), while free THC was diluted with PBS to the same concentration as the THC@NaCas nanoparticles. The different nanoparticles of THC@NaCas and free THC were mixed with 0.5 mL of L-tyrosine and kept at 37 °C for 5 min. Then 0.25 mL of tyrosinase (100 Units/mL) in PBS and 1.25 mL of PBS were added into each solution and incubated at 37 °C for 10 min with continuous agitation, following which the absorbance was measured at 475 nm [27]. Determining the inhibition of tyrosinase activity was based on the following equation [26, 28].

$$Inhibition = \frac{\mathrm{A} - \mathrm{B}}{\mathrm{A}} \times 100\%$$

A represents the absorbance of the sample, B represents the absorbance of the blank control.

3. Results and discussion

3.1. Preparation and characterization of THC@NaCas

In order to maximize the content of THC in prepared nanoparticles, we studied the influence of different concentrations of THC on the LC and EE. **Table 1** showed the LC and EE of THC by using different ratio of NaCas and free THC. When the concentration of NaCas was 1 mg/mL, the LC of THC was gradually increased from 2.30 % to 2.76 % as the increase of the concentration of THC solution. The EE of THC increased to a certain value and then began to

decline. Similar results were found at the concentration of NaCas was 2 mg/mL. When the concentrations of NaCas and THC were both 2mg/mL, it had the best LC (3.00 ± 0.26 %). We chose the condition to prepare THC@NaCas in the following research.

The surface potential and the average diameter of nanoparticles were also characterized by dynamic light scattering (DLS). The surface potential of THC@NaCas increased slightly compared with NaCas, which increased from -22.5 mV to -21.3 mV (**Table. S1**). The high surface negative potential endows THC@NaCas with high stability and good dispersion as a result of electrostatic repulsion between the particles. The particle sizes of NaCas and THC@NaCas were 263.6 nm and 269.8 nm, respectively. This result indicated that THC successfully inserted into the hydrophobic site of NaCas, so that the nanocomposite still maintain a small size.

SEM was applied to visualize the surface morphology of NaCas and THC@NaCas particles (**Fig**. **1A** and **Fig. 1B**). The morphology of NaCas was relatively uniform and spherical (Fig. 1A), which was consistent with previous reports [29]. Following the encapsulation of THC in NaCas the morphology of the THC@NaCas changed not only in shape but also in size, which agreed with the results of previously reported encapsulating experiments [30]. The morphology of the THC@NaCas showed uneven and irregular spherical and angular shapes (**Fig. 1B**). This was taken as an indication that THC was encapsulated into a NaCas casing.

X-ray diffraction (XRD) was applied to investigate the nanoparticle formation of THC encapsulation into NaCas (**Fig. 1C**). Our results revealed that pure THC displayed obvious and characteristic peaks at angles 8.16, 11.48, 14.40, 17.78, 24.02, which was consistent with a previous report [31], indicating that pure THC was in a highly crystalline form. However, no obvious peaks were detected in the XRD patterns of NaCas, displaying amorphous characteristics. The THC@NaCas scan displayed a more amorphous background with only some minor evidence of crystalline forms. The minor crystalline signals might be due to fractions of the entrapped THC protruding from the NaCas casing, which was likely to be the result of the spontaneous encapsulation of free THC by NaCas, as also described elsewhere [32]. However, the self-assembly that occurred when the THC@NaCas was formed proved that the spontaneous encapsulation shielded most of the crystalline THC from the external environment. The crystalline peaks that were observed for THC@NaCas did not line up entirely with the peak seen for pure THC, the most likely explanation for this was that the presence of the caseinate proteins caused some steric hindrance during crystal packing affecting its configurative alignment [33].

We further investigated the nanoparticle formation of the encapsulation of THC by NaCas by means of FTIR spectroscopy (**Fig. 1D**). Our results revealed changes in the secondary structure of NaCas as well as the dynamics of its interaction with THC. THC was characterized by

distinct absorption peaks at 3417 cm^{-1} and 2848 cm^{-1} (O-H stretching on the phenolic groups), 1720 cm^{-1} (C=O stretching on the diketone groups), 1614 cm^{-1}, 1000 cm^{-1} and 700 cm^{-1} (C=C bending on the aromatic rings), 1515 cm^{-1} (C=C stretching in aromatic ring), 1450 cm^{-1} (C-H bending on methyl groups) and 867 cm^{-1} (C-H bending on alkane chains), and 1300-1200 cm^{-1} (=C-O-CH_3 stretching of alkyl-aryl ether groups) [34].

NaCas was characterized by broad absorption peaks between 3500 and 2700 cm^{-1}, which included N-H stretching due to the secondary amines in the peptide bonds and C-H stretching on the peptides and a distinct peak near 3100 cm^{-1} due to amine salts, the peak position of the amide-I band of NaCas at 1740 to 1680 cm^{-1} (C=O stretching, representing an α-helix structure), and its amide-II was occurred at 1640 cm^{-1} (C-N stretching coupled with N-H bending, representing antiparallel β-sheet structures), 1520 cm^{-1} (-CH_2 shear vibration), and 1200 cm^{-1} (C-O bending) [35].

The FTIR spectrum of the THC@NaCas was broadly similar to NaCas over the range from 4000 to 2000 cm^{-1}, which represented the principle peptide related absorbances. After NaCas encapsulated THC, the peak position of NaCas for the amide-I band shifted from 1739 cm^{-1} to 1652 cm^{-1} and for the amide-II band from 1640 cm^{-1} to 1519 cm^{-1}, indicating a conformational change in the NaCas peptides due to the steric effect of THC on NaCas. Similarly, the peaks for the alkyl-aryl ether groups on THC appeared to have shifted from 1300-1200 cm^{-1} to 1100-1000

298 cm^{-1}, which reiterated the XRD results that the presence of the caseinate proteins influence the
299 molecular packing of encapsulated molecules, affecting their configurative alignment. These
300 results indicate that the formation of nanocomposites between NaCas and THC was
301 accompanied by changes in secondary structure and chemical microenvironment of both NaCas
302 and THC.

303 In order to assess whether THC has a greater overall solubility when encapsulated into
304 NaCas compared to free THC we dissolved both free THC and THC@NaCas into deionized
305 water at two different temperatures. In the subsequent phase solubility experiments (**Fig. S2**),
306 we found that the solubility of THC incorporated as THC@NaCas increased with the increase
307 of concentration at both 25 °C and 37 °C, with a greater solubility at 37 °C compared to 25 °C.
308 The solubility of THC in deionized water was calculated to be 258.3 µg/mL and 179.2 µg/mL at
309 37 °C and 25 °C respectively when the concentration of THC@NaCas suspensions were 10
310 mg/mL. The solubility of THC in THC@NaCas was 53 and 28 times higher compared to free
311 THC (3.4 µg/mL at 25 °C and 9.2 µg/mL at 37 °C). Hence, the solubility is markedly improved
312 when encapsulated into a NaCas casing, which is in agreement with findings by Park and
313 coworkers who reported similar results when encapsulating turmeric into a biodegradable
314 carrier [36].

315 **Table 1**

316 **The loading capacity and encapsulation efficiency of THC on different condition**

NaCas (mg/mL)	THC (mg/mL)	EE (%) ± SD	LC (%) ± SD
1	0.5	86.64 ± 0.67	2.30 ± 0.08
1	1	95.95 ± 0.49	2.45 ± 0.12
1	1.5	94.91 ± 0.58	2.56 ± 0.25
1	2	87.36 ± 0.89	2.76 ± 0.17
2	0.5	97.60 ± 0.73	2.47 ± 0.39
2	1	98.63 ± 1.23	2.63 ± 0.34
2	1.5	98.71 ± 0.66	2.71 ± 0.09
2	2	96.34 ± 0.23	3.00 ± 0.26

317 Abbreviation: NaCas: sodium caseinate; THC: Tetrahydrocurcumin; EE (%): encapsulation

318 efficiency; LC (%): loading capacity. All measurements are means ±SD (n=3).

319

320

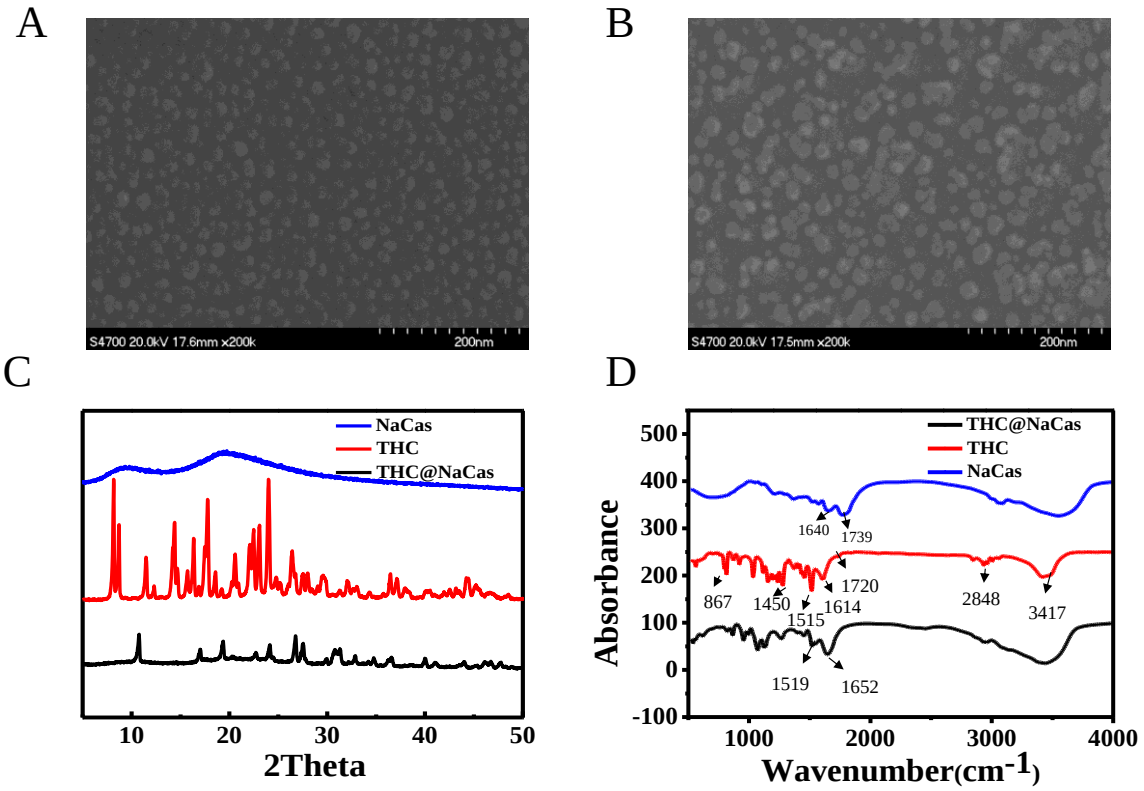

321

322 **Fig. 1**. Characterizations of nanoparticles. SEM images of (A) NaCas and (B) THC@NaCas. (C)

323 XRD spectra and (D) FTIR analysis of NaCas, THC and THC@NaCas.

324

325 ***3.2. Stability of THC@NaCas***

326 The stability of free and encapsulated THC in extreme environments was also studied, such

327 as high temperature and strong acidic conditions. Thermal stability experiment (**Fig. 3A**)

328 showed that free THC had good thermal stability. After heated at 80 ºC for 2.5 h, the

329 degradation rate of free THC was only 20 %. THC was encapsulated with NaCas not only had

330 no effect on the stability but further improvement. Free THC and THC@NaCas also could

331 maintain strong stability in different pH solution. As shown in **Fig. 3B**, THC@NaCas degraded

more slowly in phosphate buffer solution of 7.0 compared to 5.4. The instability of NaCas in acidic conditions led to the degradation rate of THC@NaCas faster than in neutral environment.

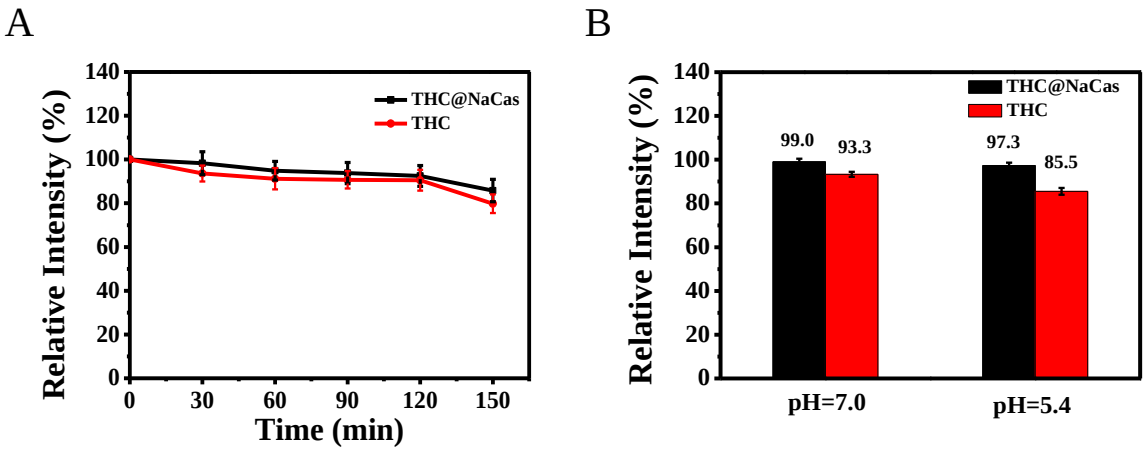

Fig. 3. The stability of free THC and THC@NaCas at 80 ºC and different pH. (A) The degradation curve of free THC and THC@NaCas at 80 ºC. (B) Retention of free THC and THC@NaCas after storage in different phosphate buffer solution (PBS) for 2 hours.

3.3. In vitro release of THC@NaCas

In order to study the release kinetics of THC from THC@NaCas in stimulate gastric fluid and normal saline, we dispersed THC@NaCas in two solutions at the same time. As shown in **Fig. 4,** the release of THC from THC@NaCas was faster in acidic gastric fluid than in normal saline. In the first 2 hours, the release of THC showed a rapid trend, the release of THC reached 45 % in stimulate gastric fluid and 40.2 % in normal saline. This might be due to some weak absorptive THC existed near the surface of sodium caseinate. Similar experimental phenomena

had also been reported in past study [37]. Subsequently, THC released more slowly and presented a slower and more lasting release pattern. The above phenomena indicated that NaCas could effectively restrain THC release from THC@NaCas. This will greatly prolong the residence time of THC in clinical application and keep lasting pharmacodynamics activity.

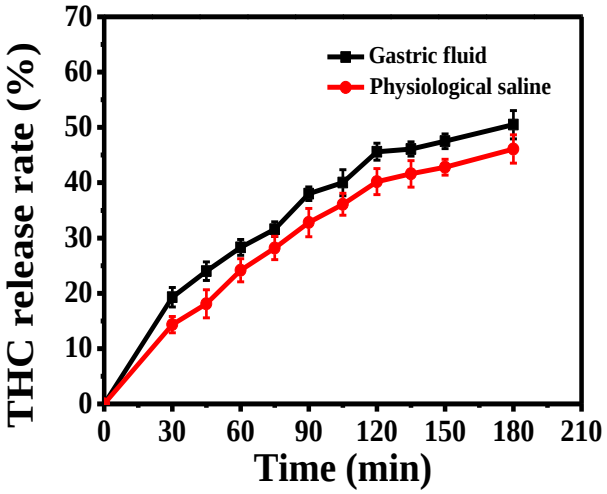

Fig. 4. The release kinetic curve of nanoparticles in stimulate gastric fluid and normal saline.

3.4. Cellular uptake of THC@NaCas

Cellular uptake capacity is an important factor for evaluating the intracellular biological activity of drugs [38]. Thus, we used confocal laser scanning microscope (CLSM) to observe the delivery of THC@NaCas in cancerous human melanoma (A375) cells. The cells were co-cultured separately with THC and THC@NaCas, while in the control group the cells were co-cultured with DMSO. The blue fluorescence visualizes the structure of A375 cells and the green fluorescence visualizes the intracellular distribution of THC in the cells. At equal

concentrations of THC, both free THC and THC@NaCas were co-cultured with A375 cells (**Fig. 5**). Encapsulated THC (THC@NaCas) showed a much more pronounced fluorescence compared to free THC, suggesting that the ability of THC to enter cells was enhanced through forming THC@NaCas. Furthermore, the rapid degradation of free THC in cancer cells could also have led to a weak fluorescence signal. Our results showed that encapsulated THC (THC@NaCas) could facilitate the stability of THC and release THC into the intracellular environment of cancer cells.

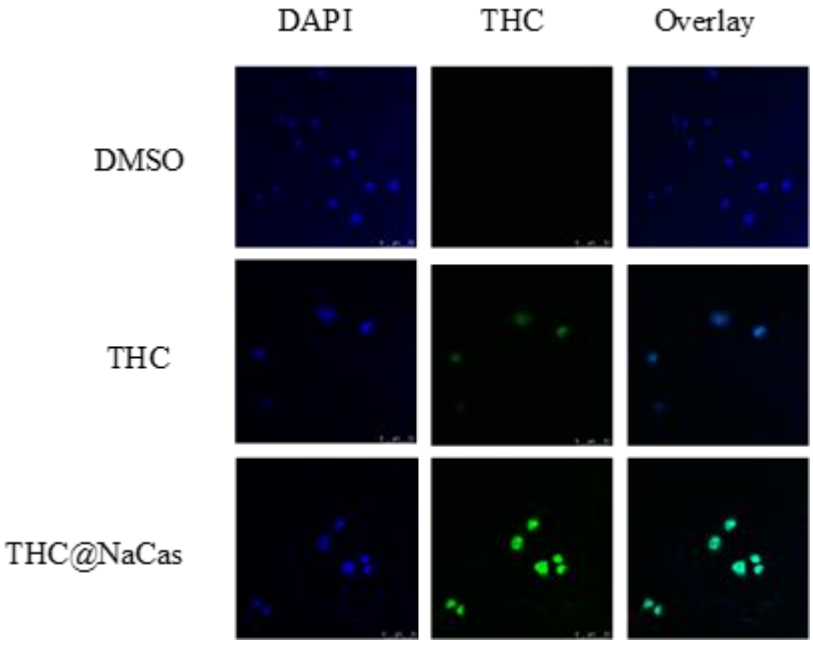

Fig. 5. Confocal laser scanning microscopy images of cancerous human melanoma (A375) cells after incubation with DMSO, THC and THC@NaCas for 4 h. (Nanoparticles: 2 μg/mL; DAPI: cell nuclear blue fluorescent probe).

3.5. Cell toxicity test

To determine the effects of THC on the survival/viability of cancerous and non-cancerous cells, in a free form and the encapsulated form (NaCas), we applied the CCK-8 assay [24]. The non-cancerous mouse embryonic cells, were not negatively affected by the presence of either free or encapsulated THC under the conditions of our experiment (**Fig. 6A**). These results suggested that THC had good biocompatibility with healthy non-melanoma cells and displayed no biological toxicity. Furthermore, THC@NaCas appeared to promote the growth of mouse embryonic cells at the lowest concentration (cell survival reached 123 % at 1 μg/mL), but the growth-stimulation effect did not persist at any of the higher THC@NaCas concentrations (c > 2 μg/mL). Free THC imposed a growth-stimulation effect on the non-cancerous mouse embryonic cells at almost all concentrations tested with an average growth stimulation at 111.2 ± 8.3% (**Fig. 6A**). This stimulatory effect might be due to the upregulation of the FOXO4 transcription factor by THC, which had been shown to linked to longevity in 3T3 cells [39].

Free THC did not inhibit the growth of cancerous human malignant melanoma cells at low concentrations, in fact growth was somewhat stimulated at concentrations up to 3 μg/ml (**Fig. 6B**). However, the growth of the malignant melanoma cells was retarded at the higher concentrations (cell viability was 95 % and 91 % at 4 and 5 μg/mL respectively). THC@NaCas

imposed an inhibitory effect on growth at almost all concentrations (**Fig. 6B**), with a very marked growth inhibition at 4 and 5 μg/mL and the cell viability was 94 % and 87 % respectively. Similar results with curcumin rather than THC were shown elsewhere [40-42], Several studies suggested that curcumin induced A375 cells apoptosis by modulating multiple signaling pathways to exert its anticancer effect and caused DNA damage in A375 cell [43, 44]. THC inhibited the growth of mouse hepatoma cells (H22 cells) by inducing mitochondrial apoptosis in previous study [45]. At present, there is no related literature report on the anticancer mechanism of THC against A375 cells.

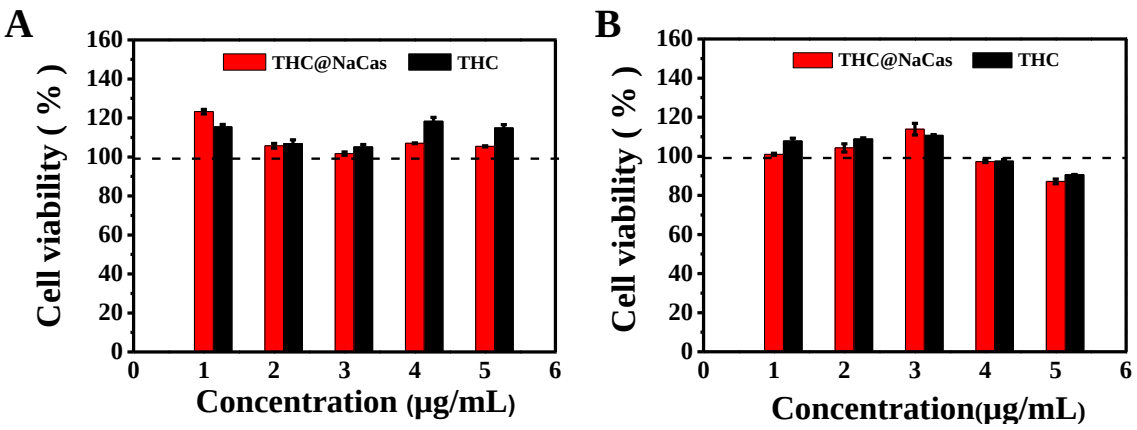

Fig. 6. Cell toxicity of THC and the THC@NaCas against mammalian cell lines at different concentrations. (A) Cell toxicity against non-cancerous mouse embryonic (3T3) cells. (B) Cell toxicity against cancerous human melanoma (A375) cells.

3.6. Cell antioxidant capacity test

To further investigate the antioxidant capabilities of THC and THC@NaCas, we adapted the

405 cellular antioxidant capacity (CAA) assay as described by Wolf and Liu [25]. The free radical
406 scavenging ability of THC can be reflected by monitoring the fluorescence intensity caused by
407 dichlorofluorescein (DCF). The principle of CAA was showed in **Scheme 1**. Mouse embryonic
408 cells (normal cells) and malignant human melanoma cells (tumor cells) were chosen as models
409 to evaluate intracellular antioxidant capacities. Our data revealed that in both cells
410 THC@NaCas had a greater ability to scavenge free radical compared to free THC (**Fig. 7A**
411 **&C**). When calculating the corresponding CAA units, it was found that the free radical
412 scavenging capacity of THC@NaCas in non-cancerous mouse embryonic cells and cancerous
413 human melanoma cells reached 29.15 and 12.58 respectively, which was 1.84 and 2.56 times of
414 the response of free THC (**Fig. 7B &D**). The elevated CAA response due to the presence of
415 THC@NaCas indicates the greater ease by which THC can be delivered into the cells,
416 regardless of whether they are cancerous cells or not. However, the reduced CAA response
417 when comparing cancerous and non-cancerous cells (regardless of whether the THC was
418 encapsulated) reiterates the possibility that THC has the ability to reduce the effective ability of
419 glutathione by depleting it [46]. Antioxidants like THC play an important role in the protection
420 against oxidative stress, especially in the case of cancer [37], more specifically THC has been
421 shown to cause a decrease in gene expression leading to anti-angiogenesis [47]. As mentioned
422 before, it appears that cancerous cells must have a greater inherent requirement for glutathione

and that even at relatively low concentrations of THC their viability is reduced.

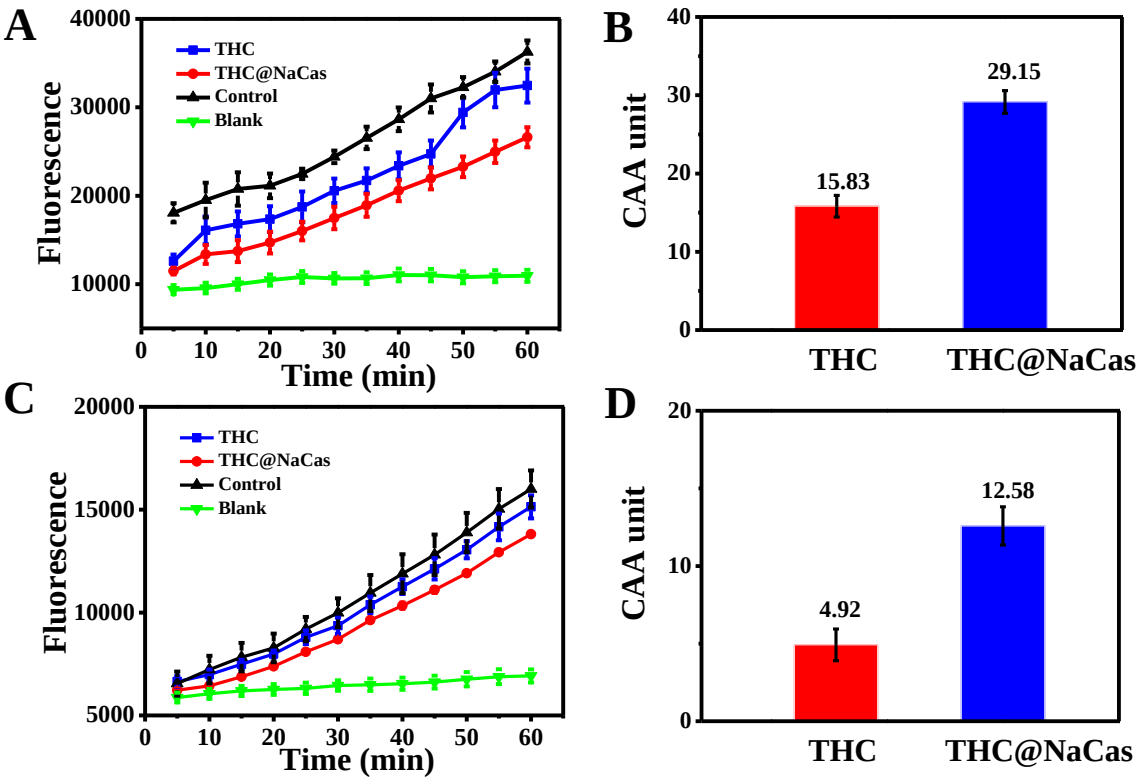

Fig. 7. The cellular antioxidant capacity of THC and the THC@NaCas. (A) Kinetics curve of DCF fluorescence from CAA of THC, THC@NaCas, control and blank sample against non-cancerous mouse embryonic (3T3) cells. (B) CAA values of THC and THC@NaCas against non-cancerous mouse embryonic (3T3) cells. (C) Kinetics curve of DCF fluorescence from CAA of THC, THC@NaCas, control and blank sample against cancerous human melanoma (A375) cells. (D) CAA values of THC and THC@NaCas against cancerous human melanoma (A375) cells.

3.7. Tyrosinase inhibition by free and encapsulated THC

THC is a known inhibitor of tyronase [26], an enzyme involved in the proliferative production of melanin. The inhibitory influence of both THC and THC@NaCas on tyrosinase was tested *in vitro*. The inhibitory effect of both free THC and THC@NaCas increased with the increase of the total concentration of THC (**Fig. 8**), however the inhibitory effect of encapsulated THC (THC@NaCas) was more pronounced compared to free THC. When the concentration of THC is 10 µg/mL, the inhibition effect of THC@NaCas is about 20 times more potent compared to free THC. Similarly, the tyronase inhibitory effect of 10 µg/mL THC as THC@NaCas was similar to the tyronase inhibitory effect at 20 µg/mL of free THC, indicating that the ultimate dose of THC could be halved if encapsulated to achieve the same inhibitory results. These results indicate that the bioavailability of encapsulated THC is markedly improved at low THC concentrations. This high tyrosinase inhibition activity might be attributed to the good dispersion and stability of encapsulated THC nanoparticles in an aqueous solution.

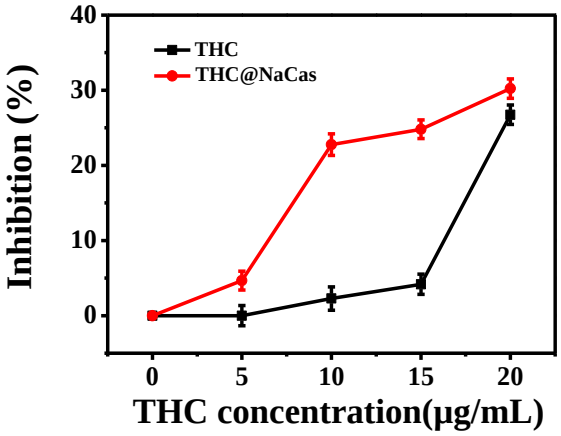

448

449 **Fig. 8.** The inhibition activity of THC and THC@NaCas on tyrosinase at different THC

450 concentration

451

452 **4. Conclution**

453 In this study, THC was successfully encapsulated in sodium caseinate to form THC@NaCas

454 nanoparticles. FTIR and XRD analyses demonstrated the THC@NaCas particles were formed

455 efficiently with the THC entrapped within a conglomerate protein matrix. The encapsulation of

456 THC in NaCas greatly improved the antioxidant activity, the cellular uptake and the inhibition

457 activity on tyrosinase of THC. Besides, the *in vitro* cytotoxicity test showed that the

458 THC@NaCas nanoparticles had inhibitory effect on cancer cells, however no inhibitory effects

459 were observed against non-cancerous cells by either free THC or THC@NaCas. Therefore, in

460 terms of clinical application perspective, THC@NaCas can be used as a safe and effective

461 anti-melanoma drug for medical treatment. In addition, it can also be used as an additive in

cosmetics, which has good antioxidant effects and have no any toxic effect on other tissues of the human body. It can be seen from our experimental results that NaCas has a strong advantage as a carrier of nano-delivery system. It can not only improve solubility and stability of hydrophobic drugs but also delay the release of drugs. Cell uptake result also shows that NaCas can enhance the cellular uptake of hydrophobic drugs. All in all, NaCas is a viable and promising candidate for the safe and effective encapsulation of THC to improve its bioavailability in clinical treatment.

Notes

The authors declare no competing financial interest.

Acknowledgements

The authors acknowledged financial support from Hebei Key Research and Development Project (20372508D) and National Natural Science Foundation of China (21878014 and 22078014).

Appendix A. Supplementary data

Supplementary data to this article can be found online.

Refernces

[1] H.N. Sun, Y. Liu, X. Bai, X.F. Zhou, H.Y. Zhou, S.J. Liu, B. Yan, Induction of oxidative stress and sensitization of cancer cells to paclitaxel by gold nanoparticles with different charge densities and hydrophobicities, J Mater Chem B 6(11) (2018) 1633-1639.

[2] P. Murugan, L. Pari, Antioxidant effect of tetrahydrocurcumin in streptozotocin-nicotinamide induced diabetic rat, Life Sci 79(18) (2006) 1720-1728.

[3] J.C. Wu, M.L. Tsai, C.S. Lai, Y.J. Wang, C.T. Ho, M.H. Pan, Chemopreventative effects of tetrahydrocurcumin on human diseases, Food Funct 5(1) (2014) 12-17.

[4] W. Song, C.M. Derito, M.K. Liu, X.J. He, M. Dong, R.H. Liu, Cellular Antioxidant Activity of Common Vegetables, J Agr Food Chem 58(11) (2010) 6621-6629.

[5] K. Pan, Y.C. Luo, Y.D. Gan, S.J. Baek, Q.X. Zhong, pH-driven encapsulation of curcumin in self-assembled casein nanoparticles for enhanced dispersibility and bioactivity, Soft Matter 10(35) (2014) 6820-6830.

[6] P. Murugan, L. Pari, Influence of tetrahydrocurcumin on erythrocyte membrane bound enzymes and antioxidant status in experimental type 2 diabetic rats, J Ethnopharmacol 113(3) (2007) 479-486.

[7] T. Plyduang, L. Lomlim, S. Yuenyongsawad, R. Wiwattanapatapee, Carboxymethylcellulose-tetrahydrocurcumin conjugates for colon-specific delivery of a novel anti-cancer agent, 4-amino tetrahydrocurcumin, Eur J Pharm Biopharm 88(2) (2014) 351-360.

[8] A. Mahal, P. Wu, Z.H. Jiang, X.Y. Wei, Schiff Bases of Tetrahydrocurcumin as Potential Anticancer Agents, Chemistryselect 4(1) (2019) 366-369.

[9] R. Lagoa, J. Silva, J.R. Rodrigues, A. Bishayee, Advances in phytochemical delivery systems for improved anticancer activity, Biotechnol Adv 38 (2020).

[10] Z. Cong, L. Zhang, S.Q. Ma, K.S. Lam, F.F. Yang, Y.H. Liao, Size-Transformable Hyaluronan Stacked Self-Assembling Peptide Nanoparticles for Improved Transcellular Tumor Penetration and Photo-Chemo Combination Therapy, ACS Nano 14(2) (2020) 1958-1970.

[11] Q. Sun, X. Sun, X. Ma, Z. Zhou, E. Jin, B. Zhang, Y. Shen, E.A. Van Kirk, W.J. Murdoch, J.R. Lott, T.P. Lodge, M. Radosz, Y. Zhao, Integration of nanoassembly functions for an effective delivery cascade for cancer drugs, Adv Mater 26(45) (2014) 7615-21.

[12] X.Y. Wang, H.M. Huang, X.Y. Chu, Y.Q. Han, M.L. Li, G.Y. Li, X.Y. Liu, Encapsulation and binding properties of curcumin in zein particles stabilized by Tween 20, Colloid Surface A 577 (2019) 274-280.

[13] D.R.B. Oliveira, G.D. Furtado, R.L. Cunha, Solid lipid nanoparticles stabilized by sodium caseinate and lactoferrin, Food Hydrocolloid 90 (2019) 321-329.

514 [14] H.R. Kavousi, M. Fathi, S.A.H. Goli, Novel cress seed mucilage and sodium caseinate
515 microparticles for encapsulation of curcumin: An approach for controlled release, Food Bioprod
516 Process 110 (2018) 126-135.
517 [15] K. Pan, H.Q. Chen, P.M. Davidson, Q.X. Zhong, Thymol Nanoencapsulated by Sodium
518 Caseinate: Physical and Antilisterial Properties, J Agr Food Chem 62(7) (2014) 1649-1657.
519 [16] I. Belyamani, F. Prochazka, G. Assezat, Production and characterization of sodium
520 caseinate edible films made by blown-film extrusion, J Food Eng 121 (2014) 39-47.
521 [17] Z. Hosseini, K. Jalili, S. Rajabnia, L. Behboodpour, F. Abbasi, Association of amphiphilic
522 block copolymers in dilute solution: With and without shear forces, J Ind Eng Chem 72 (2019)
523 319-331.
524 [18] M. Arshad, R.A. Pradhan, A. Ullah, Synthesis of lipid-based amphiphilic block copolymer
525 and its evaluation as nano drug carrier, Mat Sci Eng C-Mater 76 (2017) 217-223.
526 [19] M. Esmaili, S.M. Ghaffari, Z. Moosavi-Movahedi, M.S. Atri, A. Sharifizadeh, M. Farhadi,
527 R. Yousefi, J.M. Chobert, T. Haertle, A.A. Moosavi-Movahedi, Beta casein-micelle as a nano
528 vehicle for solubility enhancement of curcumin; food industry application, Lwt-Food Sci
529 Technol 44(10) (2011) 2166-2172.

530 [20] F.P. Chen, B.S. Li, C.H. Tang, Nanocomplexation between Curcumin and Soy Protein
531 Isolate: Influence on Curcumin Stability/Bioaccessibility and in Vitro Protein Digestibility, J
532 Agr Food Chem 63(13) (2015) 3559-3569.
533 [21] L. Luo, Y. Wu, C. Liu, Y. Zou, L. Huang, Y. Liang, J. Ren, Y. Liu, Q. Lin, Elaboration
534 and characterization of curcumin-loaded soy soluble polysaccharide (SSPS)-based nanocarriers
535 mediated by antimicrobial peptide nisin, Food Chem 336 (2021) 127669.
536 [22] Y.B. Yu, W.D. Cai, Z.W. Wang, J.K. Yan, Emulsifying properties of a ferulic acid-grafted
537 curdlan conjugate and its contribution to the chemical stability of beta-carotene, Food Chem
538 339 (2021) 128053.
539 [23] A.F. Martins, P.V. Bueno, E.A. Almeida, F.H. Rodrigues, A.F. Rubira, E.C. Muniz,
540 Characterization of N-trimethyl chitosan/alginate complexes and curcumin release, Int J Biol
541 Macromol 57 (2013) 174-84.
542 [24] F. Liao, L. Liu, E. Luo, J. Hu, Curcumin enhances anti-tumor immune response in tongue
543 squamous cell carcinoma, Arch Oral Biol 92 (2018) 32-37.
544 [25] K.L. Wolfe, R.H. Liu, Cellular antioxidant activity (CAA) assay for assessing antioxidants,
545 foods, and dietary supplements, J Agr Food Chem 55(22) (2007) 8896-8907.

546 [26] Y. Wei, F. Vriesekoop, Q. Yuan, H. Liang, beta-Lactoglobulin as a Nanotransporter for
547 Glabridin: Exploring the Binding Properties and Bioactivity Influences, ACS Omega 3(9)
548 (2018) 12246-12252.
549 [27] Z. Liu, Q. Wu, J. He, F. Vriesekoop, H. Liang, Crystal-Seeded Growth of pH-Responsive
550 Metal–Organic Frameworks for Enhancing Encapsulation, Stability, and Bioactivity of
551 Hydrophobicity Compounds, ACS Biomaterials Science & Engineering 5(12) (2019)
552 6581-6589.
553 [28] O.A.K. Khalil, O.M.M.D. Oliveira, J.C.R. Vellosa, A.U. de Quadros, L.M. Dalposso, T.K.
554 Karam, R.M. Mainardes, N.M. Khalil, Curcumin antifungal and antioxidant activities are
555 increased in the presence of ascorbic acid, Food Chem 133(3) (2012) 1001-1005.
556 [29] K. Pan, Q.X. Zhong, S.J. Baek, Enhanced Dispersibility and Bioactivity of Curcumin by
557 Encapsulation in Casein Nanocapsules, J Agr Food Chem 61(25) (2013) 6036-6043.
558 [30] L. Maldonado, R. Sadeghi, J. Kokini, Nanoparticulation of bovine serum albumin and
559 poly-d-lysine through complex coacervation and encapsulation of curcumin, Colloids Surf B
560 Biointerfaces 159 (2017) 759-769.
561 [31] Y. Zhang, F. Yao, J. Liu, W. Zhou, L.L. Yu, Synthesis and characterization of alkylated
562 caseinate, and its structure-curcumin loading property relationship in water, Food Chem 244
563 (2018) 246-253.

564 [32] T. Feng, K. Wang, F.F. Liu, R. Ye, X. Zhu, H.N. Zhuang, Z.M. Xue, Structural
565 characterization and bioavailability of ternary nanoparticles consisting of amylose,
566 alpha-linoleic acid and beta-lactoglobulin complexed with naringin, Int. J. Biol. Macromol. 99
567 (2017) 365-374.
568 [33] S. Dey, A. Schonleber, S. Mondal, S.I. Ali, S. van Smaalen, Role of Steric Hindrance in
569 the Crystal Packing of Z '=4 Superstructure of Trimethyltin Hydroxide, Cryst. Growth Des.
570 18(3) (2018) 1394-1400.
571 [34] H. Souguir, F. Salaun, P. Douillet, I. Vroman, S. Chatterjee, Nanoencapsulation of
572 curcumin in polyurethane and polyurea shells by an emulsion diffusion method, Chem Eng J
573 221 (2013) 133-145.
574 [35] T.F. Kumosinski, J.J. Unruh, Quantitation of the global secondary structure of globular
575 proteins by FTIR spectroscopy: Comparison with X-ray crystallographic structure, Talanta
576 43(2) (1996) 199-219.
577 [36] H.R. Park, S.J. Rho, Y.R. Kim, Solubility, stability, and bioaccessibility improvement of
578 curcumin encapsulated using 4-alpha-glucanotransferase-modified rice starch with reversible
579 pH-induced aggregation property, Food Hydrocolloid 95 (2019) 19-32.
580 [37] A.A. Adwa, A.S.I. Elsayed, A.E. Azab, F.A. Quwaydir, Oxidative stress and antioxidant
581 mechanisms in human body., J Appl Biotechnol Bioeng 6 (2019) 43-47.

582 [38] H. Zhang, W. Jiang, R. Liu, J. Zhang, D. Zhang, Z. Li, Y. Luan, Rational Design of Metal
583 Organic Framework Nanocarrier-Based Codelivery System of Doxorubicin
584 Hydrochloride/Verapamil Hydrochloride for Overcoming Multidrug Resistance with Efficient
585 Targeted Cancer Therapy, ACS Appl Mater Interfaces 9(23) (2017) 19687-19697.
586 [39] L. Xiang, Y. Nakamura, Y.M. Lim, Y. Yamasaki, Y. Kurokawa-Nose, W. Maruyama, T.
587 Osawa, A. Matsuura, N. Motoyama, L. Tsuda, Tetrahydrocurcumin extends life span and
588 inhibits the oxidative stress response by regulating the FOXO forkhead transcription factor,
589 Aging-Us 3 (2011) 1098-1109.
590 [40] C. Syng-ai, A.L. Kumari, A. Khar, Effect of curcumin on normal and tumor cells: Role of
591 glutathione and bcl-2, Mol Cancer Ther 3(9) (2004) 1101-1108.
592 [41] T. Choudhuri, S. Pal, T. Das, G. Sa, Curcumin selectively induces apoptosis in deregulated
593 cyclin D1-expressed cells at G(2) phase of cell cycle in a p53-dependent manner, J Biol Chem
594 280(20) (2005) 20059-20068.
595 [42] P.Y. Chang, S.F. Peng, C.Y. Lee, C.C. Lu, S.C. Tsai, T.M. Shieh, T.S. Wu, M.G. Tu, M.Y.
596 Chen, J.S. Yang, Curcumin-loaded nanoparticles induce apoptotic cell death through regulation
597 of the function of MDR1 and reactive oxygen species in cisplatin-resistant CAR human oral
598 cancer cells, Int J Oncol 43(4) (2013) 1141-1150.

599 [43] L. Bechnak, C. Khalil, R. El Kurdi, R.S. Khnayzer, D. Patra, Curcumin encapsulated
600 colloidal amphiphilic block co-polymeric nanocapsules: colloidal nanocapsules enhance
601 photodynamic and anticancer activities of curcumin, Photochemical & Photobiological
602 Sciences 19(8) (2020) 1088-1098.
603 [44] G. Zhao, X. Han, S. Zheng, Z. Li, Y. Sha, J. Ni, Z. Sun, S. Qiao, Z. Song, Curcumin
604 induces autophagy, inhibits proliferation and invasion by downregulating AKT/mTOR
605 signaling pathway in human melanoma cells, Oncol Rep 35(2) (2016) 1065-74.
606 [45] W. Liu, Z. Zhang, G. Lin, D. Luo, H. Chen, H. Yang, J. Liang, Y. Liu, J. Xie, Z. Su, H.
607 Cao, Tetrahydrocurcumin is more effective than curcumin in inducing the apoptosis of H22
608 cells via regulation of a mitochondrial apoptosis pathway in ascites tumor-bearing mice, Food
609 Funct 8(9) (2017) 3120-3129.
610 [46] S. Awasthi, U. Pandya, S.S. Singhal, J.T. Lin, V. Thiviyanathan, W.E. Seifert Jr, Y.C.
611 Awasthi, G.A.S. Ansari, Curcumin glutathione interactions and the role of human glutathione
612 S-transferas., Chemico-Biological Interaction 128 (2000) 19-38.
613 [47] P. Yoysungnoen, P. Wirachwong, C. Changtam, A. Suksamram, S. Patumraj, Anti-cancer
614 and anti-angiogenic effects of curcumin and tetrahydrocurcumin on implanted hepatocellular
615 carcinoma in nude mice, World J Gastroentero 14(13) (2008) 2003-2009.
616